

REVIEW

IN SEARCH OF A PHYSIOLOGICAL BASIS FOR COVARIATIONS IN LIGHT-LIMITED AND LIGHT-SATURATED PHOTOSYNTHESIS¹

*Michael J. Behrenfeld*²

National Aeronautics and Space Administration, Goddard Space Flight Center, Code 970, Building 22,
Greenbelt, Maryland 20771, USA

Ondrej Prasil

Institute of Microbiology, AVČR, 379 81 Třeboň/Institute of Physical Biology, University of South Bohemia,
Nové Hradky, Czech Republic

Marcel Babin

Laboratoire d'Océanographie de Villefranche, Université Pierre et Marie Curie / CNRS Quai de la Darse,
BP 806238, Villefranche-sur-Mer Cedex, France

and

Flavienne Bruyant

Dalhousie University, Department of Oceanography, Halifax, Nova Scotia B3H 4J1, Canada

The photosynthesis-irradiance (PE) relationship links indices of phytoplankton biomass (e.g. chl) to rates of primary production. The PE curve can be characterized by two variables: the light-limited slope (α^b) and the light-saturated rate (P_{\max}^b) of photosynthesis. Variability in PE curves can be separated into two categories: that associated with changes in the light saturation index, E_k ($= P_{\max}^b/\alpha^b$) and that associated with parallel changes in α^b and P_{\max}^b (i.e. no change in E_k). The former group we refer to as “ E_k -dependent” variability, and it results predominantly from photoacclimation (i.e. physiological adjustments in response to changing light). The latter group we refer to as “ E_k -independent” variability, and its physiological basis is unknown. Here, we provide the first review of the sporadic field and laboratory reports of E_k -independent variability, and then from a stepwise analysis of potential mechanisms we propose that this important yet largely neglected phenomenon results from growth rate-dependent variability in the metabolic processing of photosynthetically generated reductants (and generally not from changes in the oxygen-evolving PSII complexes). Specifically, we suggest that as growth rates decrease (e.g. due to nutrient stress), reductants are increasingly used for simple ATP generation through a fast (<1s) respiratory pathway that skips the carbon reduction cycle altogether and is undetected by standard PE methodologies. The proposed mechanism is con-

sistent with the field and laboratory data and involves a simple new “twist” on established metabolic pathways. Our conclusions emphasize that simple reductants, not reduced carbon compounds, are the central currency of photoautotrophs.

Key index words: photosynthesis-irradiance relationships, productivity, phytoplankton, physiology

Abbreviations: DHAP, dihydroxyacetone phosphate; GAP, glyceraldehyde 3-phosphate; OAA, oxaloacetate; PE, photosynthesis-irradiance; PGA, phosphoglyceric acid; PQ, plastoquinone; RuBP, ribulose-1,5 bisphosphate

Despite the myriad field and laboratory studies conducted and the many insights gained in the past century on algal physiology, mechanisms underlying a variety of first-order phenomena remain unresolved. Unraveling these biological “mysteries” may require the discovery of novel biochemical processes or may simply require new insights on interactions between pathways already understood. One of these mysteries, and the focus of this review, is the frequently observed positive correlation between the light-limited slope (α^b) and light-saturated rate (P_{\max}^b) of photosynthesis. The implications of this phenomenon on light-photosynthesis relationships are, at the very least, comparable in magnitude to photoacclimation. Nevertheless, covariability in α^b and P_{\max}^b has received relatively little attention, a review on the topic has never been written, and the physiological basis has remained “at large.” In

¹Received 30 April 2003. Accepted 23 October 2003.

²Author for correspondence: e-mail mjb@neptune.gsfc.nasa.gov.

the following pages, we attempt to address these issues by 1) formalizing the “positive correlation” problem, 2) collating the fragmented field and laboratory data available, 3) reviewing potentially relevant photosynthetic and metabolic pathways, and 4) proposing a physiological explanation for the phenomenon. We hope that through this review and suggested primary mechanism, this effort will stimulate a resurgence of investigation into this important form of variability in algal photosynthesis-irradiance (PE) relationships.

LIGHT-PHOTOSYNTHESIS RELATIONSHIPS: TWO CATEGORIES OF VARIABILITY

For a given algal suspension, the relationship between light and photosynthesis exhibits a predictable shape (the PE curve). At the lowest light levels, photosynthesis is a linear function of irradiance (Fig. 1, Table 1) with a slope that can be described as either a function of incident (α) or absorbed light (Φ_{\max}). With further increases in light, photosynthetic yield per light quanta absorbed decreases in a manner generally following a Poisson function. Photosynthesis eventually becomes light-saturated (P_{\max}) and then remains unchanged with additional light (Fig. 1), unless significant photoinhibition occurs. Behavior of the PE curve is dependent in part on whether photosynthesis is normalized to cell abundance, total cell volume, carbon biomass, or chl concentration (MacIntyre et al. 2002).

When normalized to cell abundance or volume, α varies with the summed light-harvesting capacity of the photosynthetic units. Because pigment content is a measure of light-harvesting capacity, a relatively constant value for the light-limited slope is anticipated upon normalization to chl concentration (α^b), particularly when chl is the primary light-harvesting pigment and the ratio of PSI to PSII is invariant. Results from algal photoacclimation studies have long confirmed a conserved nature to α^b (Steemann Nielsen and Jørgensen 1968), thereby justifying this basic assumption in dynamic phytoplankton acclimation models (Geider et al. 1996, 1998). Changes in light-harvesting complexes that are known to alter α^b at different time scales include nonphotochemical quenching, the concentration of photosynthetically active accessory pigments (due to the smaller fraction of absorption attributed to chl), the PSI:PSII ratio, and photoinhibition.

Under most conditions, light-saturated photosynthesis (P_{\max}) appears to be limited by processes “downstream” of PSII (Kok 1956, Weinbaum et al. 1979, Heber et al. 1988, Leverenz et al. 1990, Behrenfeld et al. 1998). In a variety of studies, P_{\max} has been found to covary with the concentration and/or activity of the Calvin cycle enzyme, RUBISCO (Björkman 1981, Sukenik et al. 1987, Rivkin 1990, Orellana and Perry 1992, Geider and McIntyre 2002), whereas in other studies P_{\max} seems to be better correlated with the photosynthetic electron transport components (Fleischhacker and Senger 1978, Wilhelm and Wild 1984, Morales et al. 1991). One condition that can result in a close

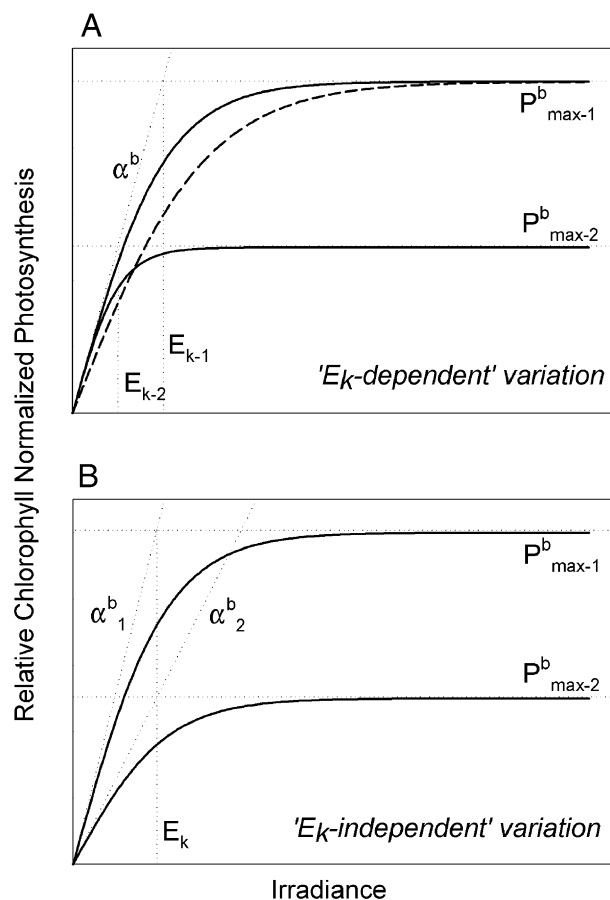


FIG. 1. The two categories of variability in chl-normalized photosynthesis-irradiance (PE) relationships. (A) E_k -dependent variations involve independent changes in the light-saturated rate, P_{\max}^b , and the light-limited slope, α^b , such that a shift occurs in the light-saturation index, $E_k = P_{\max}^b/\alpha^b$. Here, the difference between the two solid lines might represent growth at high ($P_{\max-1}^b$ and E_{k-1}) and low ($P_{\max-2}^b$ and E_{k-2}) light. This process of photoacclimation need not alter α^b if pigment composition and photoinhibition are unaffected. If photoinhibition were pronounced under high light (represented by the dashed line), it would cause a decrease in α^b without necessarily altering P_{\max}^b (Behrenfeld et al. 1998). (B) E_k -independent variability involves parallel changes in P_{\max}^b and α^b , such that E_k remains essentially unaltered (in this figure, the two PE curves are characterized by the variable sets, $\{P_{\max-1}^b, \alpha_1^b, E_k\}$ and $\{P_{\max-2}^b, \alpha_2^b, E_k\}$). As described in the text, significant E_k -independent variability has been sporadically reported from field studies since its original description by Platt and Jassby (1976). Similar variability has also been observed in the laboratory over the diel cycle. The physiological basis for this class of PE variability has remained unresolved.

coupling between PSII capacity and P_{\max} is acclimation to very high light (Behrenfeld et al. 1998, figs. 4 and 5; but note that their x -axes in both A panels should read “irradiance”). However, P_{\max} responds very differently to a change in growth irradiance than does light-harvesting capacity (Sukenik et al. 1987, Behrenfeld et al. 2002b). Consequently, photoacclimation (the physiological response to changes in light) has a pronounced influence on the chl-normalized light-saturated photosynthetic rate (P_{\max}^b) (Fig. 1A).

TABLE 1. Definitions, abbreviations, and notations.

Name	Definition	Unit example
Photosynthesis-irradiance (PE) curves		
α	Light-limited slope of the PE curve	$\text{mg C} \cdot \text{m}^2 \cdot \text{s} \cdot (\text{L} \cdot \text{h} \cdot \mu\text{mol quanta})^{-1}$
Φ_{max}	Absorption-based light-limited slope of PE curve	$\text{mol C} \cdot (\text{mol quanta absorbed})^{-1}$
α^b	α normalized to chl concentration	$\text{mg C} \cdot \text{m}^2 \cdot \text{s} \cdot (\text{mg chl} \cdot \text{h} \cdot \mu\text{mol quanta})^{-1}$
P_{max}	Light-saturated rate of photosynthesis	$\text{mg C} \cdot \text{L}^{-1} \cdot \text{h}^{-1}$
P_{max}^*	Absorption-normalized P_{max}	$\text{mol C} \cdot \text{m}^{-2} \cdot \text{h}^{-1}$
P_{max}^b	Chl-normalized P_{max}	$\text{mg C} \cdot \text{mg chl}^{-1} \cdot \text{h}^{-1}$
E_k	Light-saturation index = P_{max}/α	$\mu\text{mol quanta} \cdot \text{m}^{-2} \cdot \text{s}$
\bar{a}^*	Chl-specific particulate absorption coefficient	$\text{m}^2 \cdot \text{mg chl}^{-1}$
Photochemistry		
PSII	Oxygen-evolving PSII complex	
PSI	PSI complex	
n_{PSII}	Concentration of PSII complexes	
n_{PSI}	Concentration of PSI complexes	
f_{PSII}	Fraction of PSII complexes that is photochemically functional	
σ_{PSII}	Functional absorption cross-section of PSII	
$\alpha_{\text{PSII}}^{\text{chl}}$	Light-limited slope for electron transport from H ₂ O to the acceptor side of PSII	
$\text{chl}/_{\text{PSII}}$	Average chl concentration per PSII	
$\text{chl}/_{\text{PSI}}$	Average chl concentration per PSI	
a_{PSII}	Optical absorption cross-section of PSII	
Φ_P	Quantum efficiency for PSII photochemistry	
Φ_F	Quantum efficiency for PSII fluorescence	
Φ_H	Quantum efficiency for PSII nonphotochemical quenching (i.e. heat dissipation)	
α_{PSII}^b	Chl-normalized α_{PSII}	
$P_{\text{m-PSII}}$	Light-saturated rate of electron transport from H ₂ O to the acceptor side of PSII	
τ_{PSII}^*	Light-saturated electron turnover rate per functional PSII	
$P_{\text{m-PSII}}^b$	Chl-normalized $P_{\text{m-PSII}}$	
n_{LF}	Concentration of the rate-limiting photosynthetic component at light saturation	
τ_{LF}	Electron turnover rate of rate-limiting component at light saturation	
F_0	Dark-adapted initial fluorescence	
F_m	Light-saturated maximum fluorescence	
F_v	Variable fluorescence = $F_m - F_0$	

Photosynthesis-irradiance relationships exhibit a tremendous degree of variability that can be separated into two basic categories according to associated changes in the light-saturation index, $E_k = P_{\text{max}}^b/\alpha^b$ (Talling 1957). Photoacclimation belongs to a category we term “ E_k -dependent” variability, because it is associated with independent changes in α^b and P_{max}^b that alter E_k (Fig. 1A). Our second category is “ E_k -independent” variability, and it involves parallel changes in α^b and P_{max}^b that have little or no influence on E_k (Fig. 1B). E_k -independent changes are wholly unexpected if, as generally assumed, α and P_{max} are limited by separate aspects of photosynthesis and α^b is relatively constant. Nevertheless, significant E_k -independent variability has been observed both in the field and in the laboratory. Before reviewing these field and laboratory results, a case study is presented in the following section to illustrate E_k -independent variability and its cooccurrence in the field with E_k -dependent changes.

OLIPAC: A CASE STUDY

The OliPac study was conducted in 1994 between 16°S, 150°W and 1°N, 150°W as part of the French program, Étude de Processus dans l’Océan Pacifique Equatorial (Dandonneau 1999). Measurements included enumeration and growth rate estimates of *Synechococcus*, *Prochlorococcus*, and picoeukaryotes (Liu et al. 1999, Vaultot and Marie 1999), PE relationships

(Babin et al. 1994, Behrenfeld et al. 1998), algal absorption spectra (\bar{a}^*) (Allali et al. 1997), variable fluorescence (Behrenfeld et al. 1998), water column density (Claustre et al. 1999), and macronutrient concentrations (Raimbault et al. 1999). The southern end of the transect was characterized by low nitrogen (NO_3^- , NO_2^- , and $\text{NH}_4^+ < 10$ nM) and chl ($< 0.1 \text{ mg} \cdot \text{m}^{-3}$) in the upper euphotic layer, relatively high dawn and dusk photochemical quantum efficiencies ($F_v/F_m \sim 0.6$, where F_v is the difference between initial [F_0] and maximal [F_m] fluorescence), and algal assemblages dominated by *Prochlorococcus* (Behrenfeld et al. 1998, Claustre et al. 1999, Vaultot and Marie 1999). The contribution of *Synechococcus* to algal biomass was greatest in the central portion of the transect, whereas picoeukaryotes were most abundant near the equator (Vaultot and Marie 1999). Dawn and dusk F_v/F_m was ~ 0.3 in the central region and ~ 0.4 near the equator. Large (35%–55%) nocturnal decreases in F_v/F_m observed between 13°S and 1°N and coincident increases in surface nitrogen to $> 2 \mu\text{M}$ near the equator (Claustre et al. 1999) indicated a prevalence of iron-limiting conditions (Behrenfeld and Kolber 1999). Surface chl concentrations ranged from $0.05 \text{ mg} \cdot \text{m}^{-3}$ at 16°S to $\sim 0.3 \text{ mg} \cdot \text{m}^{-3}$ at 1°N. Across the entire transect, diurnal stratification resulted in midday surface photoinhibition that decreased with depth paralleling the attenuation of light (Behrenfeld et al. 1998).

During OliPac, 159 PE curves were determined using samples collected between 5 m and 150 m depth. P_{\max}^b ranged from 0.07 to 4.54 mg C · mg chl⁻¹ · h⁻¹ and α^b ranged from 0.0014 to 0.12 mg C · m² · s · (mg chl · h · μmol quanta)⁻¹. Because stratification was persistent throughout the transect, depth-dependent changes in photoacclimation could be accounted for by separating the PE data into optical depth bins (optical depth = sample depth × mean attenuation coefficient [k_d] for PAR). Regression analysis of data in each optical depth bin revealed strong correlations between α^b and P_{\max}^b ($0.42 < r^2 < 0.93$). A potential explanation for these parallel changes is that they reflected variability in accessory pigments. Specifically, if two populations have the same α and P_{\max} but one gathers 50% of its light using accessory pigments whereas the other exclusively uses chl, then the former will have a factor of 2 higher P_{\max}^b and α^b simply due to division by a lower chl concentration.

The contribution of accessory pigments to PE variability can be accounted for by dividing P_{\max}^b and α^b by the chl-specific particulate absorption coefficients (\bar{a}^*), which ranged from 0.0069 to 0.049 m² · mg chl⁻¹ during OliPac. Resultant maximum quantum yields ($\Phi_{\max} = \alpha^b / \bar{a}^*$) ranged from 0.001 to 0.101 · mol C · (mol quanta absorbed)⁻¹, whereas absorption-based light-saturated photosynthetic rates ($P_{\max}^* = P_{\max}^b / \bar{a}^*$) varied from 0.038 to 3.62 mol C · m⁻² · h⁻¹. Within each optical depth bin, Φ_{\max} and P_{\max}^* remained highly correlated ($0.50 < r^2 < 0.95$) (Fig. 2, A–I). This result demonstrates that, at least in the case of OliPac, variability in \bar{a}^* plays a minor role in E_k -independent variations of the PE relationship.

Although the within-bin correlations in Φ_{\max} and P_{\max}^* illustrate E_k -independent variability, the between-bin changes in slope represent E_k -dependent variability (Fig. 2, A–I). From the surface to ~2 optical depths, changes in E_k could be entirely accounted for by photoinhibitory losses of functional PSII (Fig. 2J), whereas at greater depths coincident decreases in P_{\max} were apparently also important (Fig. 2K). A decrease in P_{\max} at growth-limiting light levels is consistent with results from Rivkin (1990) and Behrenfeld et al. (2002a). The E_k -dependent changes observed during OliPac are thus consistent with established responses to growth irradiance. In contrast, we found the E_k -independent variability to be unexplained by \bar{a}^* , temperature, salinity, nitrate, PSII functional absorption cross-sections (σ_{PSII}), or the concentration of *Prochlorococcus*, *Synechococcus*, or picoeukaryotes. A similar conundrum has been repeatedly experienced in field studies since the introduction of the problem by Platt and Jassby in 1976, as detailed in the following review section.

HISTORICAL FIELD OBSERVATIONS OF E_k -INDEPENDENT VARIABILITY

The pioneering work of Platt and Jassby (1976) was based on an analysis of PE data collected at three coastal

locations off Nova Scotia, Canada between July 1973 and March 1975. In addition to the 188 PE experiments conducted on samples collected from 1 to 10 · m depth, measurements were also made of chl concentration, surface irradiance, and temperature. For the entire data set, α^b and P_{\max}^b covaried ($r^2 = 0.64$). This relationship is illustrated in Figure 3A for the subset of data collected in St. Margaret's Bay ($r^2 = 0.44$; $n = 106$; $0.03 \leq \alpha^b \leq 0.63$ mg C · m² · (mg chl · h · W)⁻¹; $0.5 \leq P_{\max}^b \leq 18.8$ · mg C · (mg chl · h)⁻¹) (data from Platt and Jassby 1976, figures 2 and 3). Platt and Jassby found that for data collected at 1 m depth, a significant correlation existed between α^b and daily PAR averaged over the 3 days before sampling ($r^2 = 0.40$) and between P_{\max}^b and temperature ($r^2 = 0.53$) (their table 6). They also noted that higher values of α^b and P_{\max}^b were associated with higher values of respiration per unit chl.

In this original report, some of the fundamental issues regarding the positive correlation between α^b and P_{\max}^b were discussed. Platt and Jassby (1976) specifically noted that α^b and P_{\max}^b should be expected *a priori* to vary independently because the former is limited by the light reactions of photosynthesis, whereas the latter is limited by the dark reactions of the Calvin cycle. They also commented on the surprising degree of variability in α^b :

The hypothesis that α^b should be more or less constant since it is a function of basic photochemical reactions which may be independent of phylogeny and, incidentally, independent of temperature is not supported by our results. (p. 424)

The authors concluded that variability in α^b and P_{\max}^b was largely driven by factors not measured during their study, with specific reference to nutrient availability and taxonomy. These two concepts were later revisited by the lead author (Coté and Platt 1983, Platt et al. 1992).

The follow-up study of Coté and Platt (1983) entailed a much more diverse suite of supporting observations. During this study, daily samples were collected from 5 m depth in Bedford Basin, Nova Scotia over a 70-day period from 18 May to 26 July 1975. Measurements included PE experiments, *in situ* temperature, surface PAR, salinity, macronutrients (NO_3^- , NO_2^- , NH_4^+ , SiO_4^{+} , PO_4^{3+}), surface winds, mean cell volume, chl concentration, particulate organic carbon and nitrogen, pheopigments, ATP, and phytoplankton taxa. For the entire study, α^b varied from ~0.07 to 0.26 mg C · m² · (mg chl · h · W)⁻¹ and P_{\max}^b varied from ~2.3 to 8.2 mg C · (mg chl · h)⁻¹. Coté and Platt (1983) partitioned the time course of their study into seven segments based on the relationship of α^b and P_{\max}^b to chl. Except for the first (18 May to 1 June) and fifth (8–16 July) periods, significant within-period correlations existed between α^b and P_{\max}^b ($0.56 < r^2 < 0.95$). Although regression slopes indicated considerable changes in E_k between periods, the combined data set retained a positive correlation

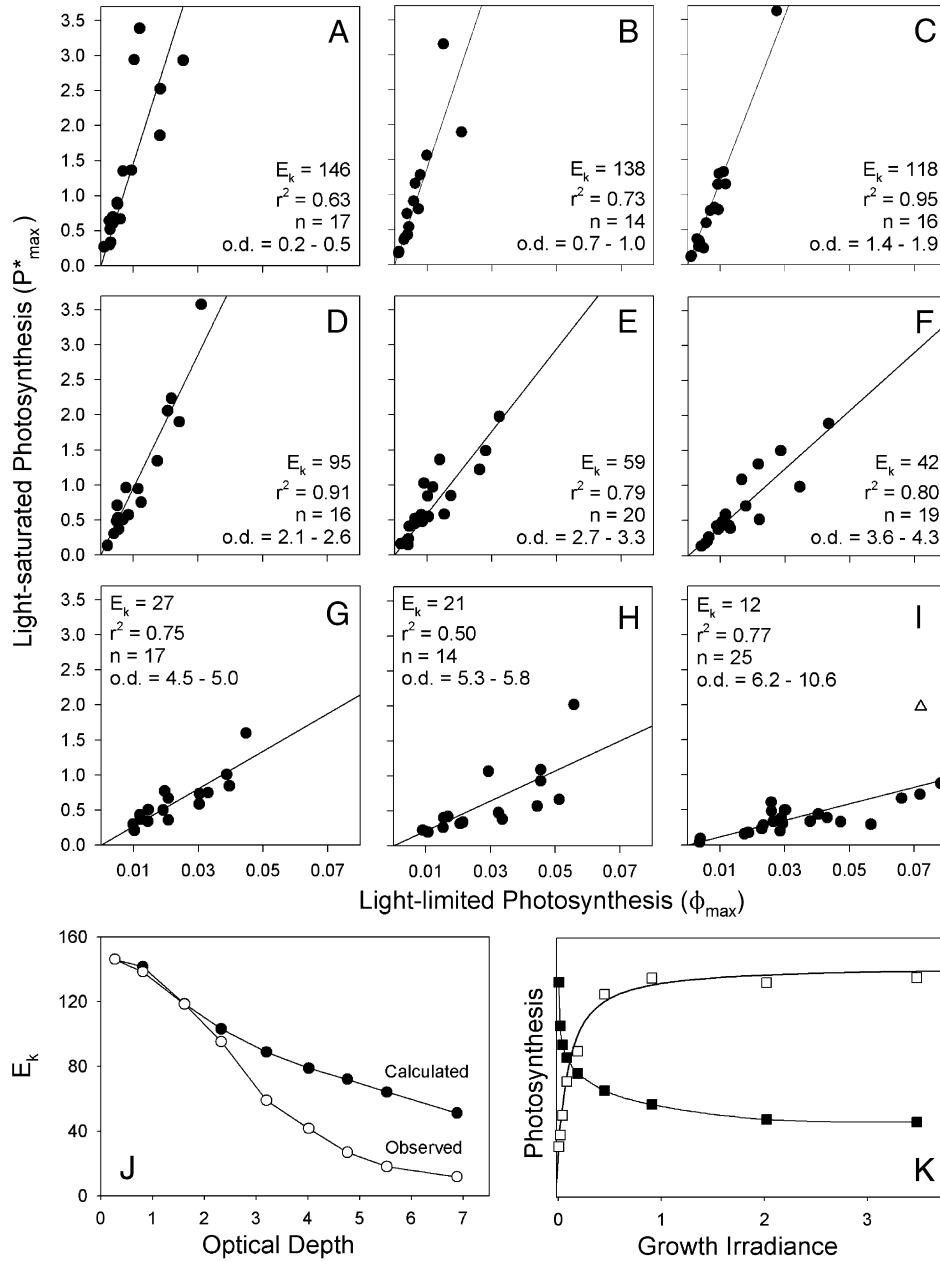


FIG. 2. Variability in photosynthesis-irradiance (PE) relationships during the 1994 OliPac study (Dandonneau 1999). (A–I) For each PE curve, an absorption-based light-limited slope (Φ_{\max} : mol C · (mol quanta absorbed)⁻¹) and light-saturated rate (P_{\max}^* : mol C · m⁻² · h⁻¹) was calculated. Data were grouped into optical depth bins (o.d. range indicated in each panel) to roughly account for E_k -dependent variability with depth. In each bin, a strong positive correlation between Φ_{\max} and P_{\max}^* is apparent (coefficient of determination [r^2] and sample number [n] are indicated in each panel). This within-bin E_k -independent variability is nearly identical to that observed in the chl-normalized PE data (α^b and P_{\max}^b), but absorption-based values are given here to illustrate that the phenomenon is not due to changes in pigment composition. (J) Changes in the light-saturation index, E_k ($= P_{\max}^*/\Phi_{\max}$), as a function of the median optical depth for each data bin (A–I). Open circles, observed E_k taken as the linear regression slope for each data set as given in panels A to I. Closed circles, calculated changes in E_k resulting from PSII-based variability in Φ_{\max} , estimated as a linear function of depth-dependent changes in F_w/F_0 (Crofts et al. 1993). (K) Relative changes in (closed squares) Φ_{\max} and (open squares) P_{\max} as a function of growth irradiance. Changes in Φ_{\max} are from J. The difference between calculated and observed E_k in J is assigned to depth-dependent changes in P_{\max} . The resultant low-light decrease in P_{\max} is consistent with independent laboratory (Rivkin 1990) and field (Behrenfeld et al. 2002b) results. Growth irradiance was calculated as the average daily PAR (400–700 mol quanta · m⁻² · d⁻¹) for a given optical depth bin.

between α^b and P_{\max}^b ($r^2 = 0.61$) as long as period 1 was excluded (Fig. 3B).

Coté and Platt (1983) conducted an extensive analysis of the combined data from periods 3 and 5

to 7 (11 June to 2 July and 8–26 July) in an attempt to identify potential sources of physiological variability. A good correlation between α^b and P_{\max}^b was reported for this combined data set ($r^2 = 0.80$; $n = 41$). Changes in

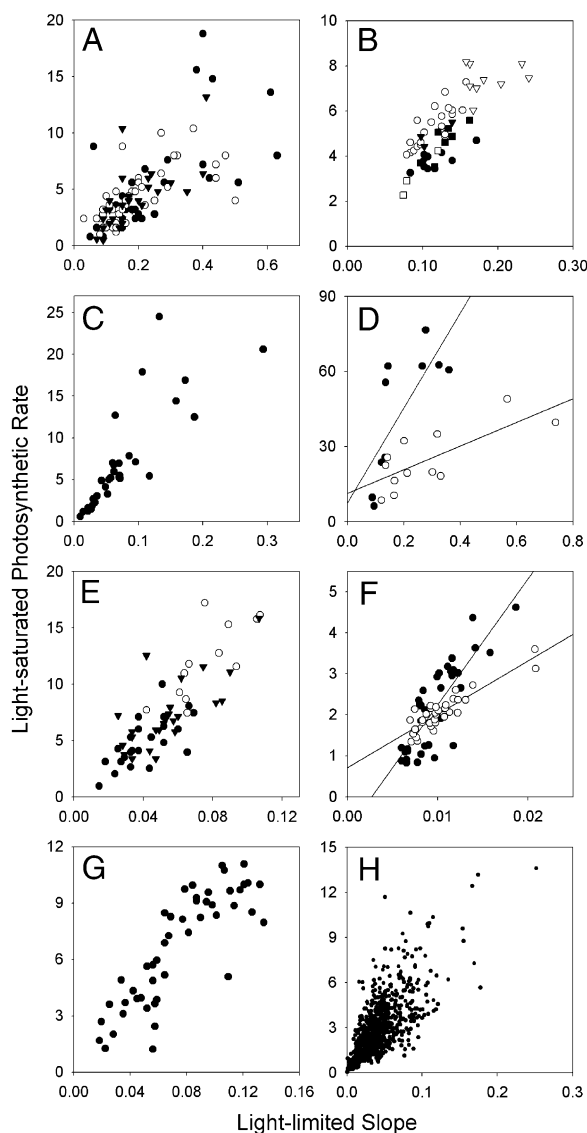


FIG. 3. Historical field data sets exhibiting positive correlations between chl-normalized light-limited slopes (α^b) and light-saturated rates (P_{\max}^b) of photosynthesis. Data sources and locations are as follows: (A) Platt and Jassby (1976), coastal Nova Scotia (closed circles, 1 m; open circles, 5 m; inverted triangles, 10 m), (B) Coté and Platt (1983), Bedford Basin, Nova Scotia (closed circles, 11 June to 2 July; open circles, 8 to 16 July; inverted triangles, 17 to 23 July; open inverted triangles, 24 to 26 July, 1975), (C) Harding et al. (1982), coastal California, (D) Harding et al. (1987), *Prorocentrum mariae-lebouriae* from the Chesapeake Bay (closed circles, surface; open circles, subpycnocline), (E) Forbes et al. (1986), coastal British Columbia (closed circles, Saanich Inlet; open circles, Strait of Georgia; inverted triangles, Hecate Strait), (F) Erga and Skjoldal (1990), Lindås-pollene, Norway (closed circles, 0.5 m; open circles, 10 m), (G) Platt et al. (1992), North Sargasso Sea (closed circles ≤ 20 m), (H) Moline et al. (1998), Antarctic Peninsula shelf. Units for α^b and P_{\max}^b differ between panels and are provided in the text.

both α^b and P_{\max}^b were negatively correlated ($r^2 = 0.72$ and 0.76 , respectively) with changes in mean cell volume, suggesting an importance of taxonomic composition. However, a consistent relationship be-

tween α^b or P_{\max}^b and species composition was not achieved, despite supporting microscopic identifications. The inverse relationship between cell volume and the PE variables was suggested to reflect an influence of cell size on nutrient uptake bestowed by changes in surface-to-volume ratios. In addition to cell size, α^b and P_{\max}^b were correlated with changes in pheopigment-to-chl ratios ($r^2 = 0.76$ and 0.86 , respectively). This ratio was taken as an index of grazing pressure on the phytoplankton crop or, more specifically, of the availability of recycled nutrients to support algal growth. The authors argued that despite measurable NO_3^- and NH_4^+ concentrations during a bulk of the study period, trophic regeneration of nutrients was critical for achieving high photosynthetic efficiencies. Thus, the authors proposed a link between nutrients and their two variables significantly correlated with changes in PE parameters. Coté and Platt also noted that upon completion of their study, significant covariations in α^b and P_{\max}^b had been documented for time scales ranging from diel, to daily, to seasonal, and at all time scales variability in α^b was much greater than predicted from physiological considerations based on photochemistry alone.

In a series of studies by Harding and coworkers (1982, 1985, 1986, 1987), synchronized changes in α^b and P_{\max}^b were observed on diel to seasonal time scales in samples collected from coastal and in-land waters of the United States. In their initial field study on mixed layer phytoplankton from the California coast (Harding et al. 1982), α^b varied from ~ 0.01 to $0.30 \mu\text{g C} \cdot \text{m}^2 \cdot \text{s} \cdot (\mu\text{g chl} \cdot \text{h} \cdot \mu\text{mol quanta})^{-1}$ and P_{\max}^b varied from ~ 0.5 to $24.3 \mu\text{g C} \cdot (\mu\text{g chl} \cdot \text{h})^{-1}$. Changes in α^b and P_{\max}^b were highly correlated ($r^2 = 0.68$; $n = 31$) (Fig. 3C) and exhibited clear diel periodicity that mimicked patterns observed in earlier laboratory experiments. The physiological basis for these cycles was not resolved but suggested to reflect true circadian rhythms (based on results of Hastings et al. [1961] and Palmer et al. [1964]). Additional studies conducted during 1982 and 1983 in the Chesapeake and Delaware Bays (Harding et al. 1986, 1987) also yielded significant correlations between α^b and P_{\max}^b ($0.28 \leq r^2 \leq 0.94$; median 0.68). Regression slopes for these correlations varied with season and sampling depth ($58 \leq E_k \leq 470$; median = $140 \mu\text{mol quanta} \cdot \text{m}^{-2} \cdot \text{s}^{-1}$).

Perhaps one of the more significant field-based contributions toward constraining the potential mechanism(s) underlying covariations in α^b and P_{\max}^b was provided by Harding et al. (1987). They described seasonal changes in PE parameters for monospecific suspensions of the red tide alga, *Prorocentrum mariae-lebouriae*, collected from within the surface mixed layer and below the pycnocline in the Chesapeake Bay. Over the course of the study, α varied from 0.09 to $0.74 \mu\text{g C} \cdot \text{m}^2 \cdot \text{s} \cdot (\text{cell} \cdot \text{h} \cdot \mu\text{mol quanta})^{-1}$ and P_{\max} varied from 7.1 to $87.1 \mu\text{g C} \cdot (\text{cell} \cdot \text{h})^{-1}$, with significant positive correlations both above and below the pycnocline ($r^2 = 0.58$ and 0.52 , respectively) (Fig. 3D). The

importance of this result was its clear demonstration that seasonal E_k -independent variability did not require taxonomic changes but could occur over a range of time scales within a single species.

Coté and Platt (1983) suggested that the correlation between α^b and P_{\max}^b may allow one variable to be better predicted given information on changes in the other. In this vein, Forbes et al. (1986) investigated how covariations in PE parameters might influence uncertainties in water-column production estimates arising from predictions based solely on P_{\max}^b . Their analysis was based on field studies conducted in coastal waters of British Columbia, Canada and at ocean station PAPA between 1983 and 1984. For their combined data set, α^b varied from ~ 0.01 to $0.11 \text{ mg C} \cdot \text{m}^2 \cdot \text{s} \cdot (\text{mg chl} \cdot \text{h} \cdot \mu\text{mol quanta})^{-1}$ and P_{\max}^b varied from ~ 1.0 to $17.2 \text{ mg C} \cdot (\text{mg chl} \cdot \text{h})^{-1}$, with a clear positive correlation between the two variables ($r^2 = 0.84$, $n = 61$) (Fig. 3E). Significant correlations between α^b and P_{\max}^b were also observed within individual data sets collected from the Strait of Georgia ($r^2 = 0.69$, $n = 13$), Saanich Inlet ($r^2 = 0.68$, $n = 24$), and Hecate Strait ($r^2 = 0.76$, $n = 24$) (Fig. 3E). The authors placed little emphasis on unraveling the physiological basis for such E_k -independent variability but did suggest that community structure played a major role through taxonomic variability in photoadaptive responses.

Transcendence of the positive correlation across time scales was noted first by Coté and Platt (1983) and Harding et al. (1987). In a later study by Erga and Skjoldal (1990), hourly to daily changes in photosynthetic parameters were followed in surface phytoplankton assemblages collected during midsummer (7–12 June 1982) in Lindåspollene, a land-locked fjord of Norway. The observed range for α^b was ~ 0.006 to $0.021 \text{ mg C} \cdot \text{m}^2 \cdot \text{s} \cdot (\text{mg chl} \cdot \text{h} \cdot \mu\text{mol quanta})^{-1}$, whereas P_{\max}^b ranged from ~ 0.8 to $4.6 \text{ mg C} \cdot (\text{mg chl} \cdot \text{h})^{-1}$. In accordance with temporal patterns observed since the original study by Doty and Oguri (1957), α^b and P_{\max}^b exhibited significant diel oscillations, with maxima in morning hours and minima in late evening. Erga and Skjoldal suggested that the morning peak in photosynthetic performance may reflect enhanced metabolic processes associated with the assimilation of nutrients accumulated during the preceding dark period. NO_3^- and PO_4^{3-} concentrations were $\leq 0.1 \mu\text{M}$ throughout their study. For the combined data, α^b and P_{\max}^b were well correlated in samples collected at 0.5 m ($r^2 = 0.70$, $n = 35$) and 10 m ($r^2 = 0.80$, $n = 33$), although regression slopes were clearly divergent between depths (Fig. 3F).

Another important contribution toward identifying forcing factors responsible for E_k -independent variability came from a series of open ocean cruises in the North Sargasso Sea (Platt et al. 1992). For the 152 PE curves measured during six cruises between 1983 and 1990, α^b ranged from ~ 0.01 to $0.19 \text{ mg C} \cdot \text{m}^2 \cdot (\text{mg chl} \cdot \text{h} \cdot \text{W})^{-1}$ and P_{\max}^b ranged from ~ 0.3 to $11.1 \text{ mg C} \cdot (\text{mg chl} \cdot \text{h})^{-1}$. Covariation in α^b and P_{\max}^b was greatest in samples collected within the upper 20 m of

the water column, with a reported coefficient of determination of $r^2 = 0.95$ ($n = 49$) (Fig. 3G). A slightly lower, but still significant correlation was reported for the full data set ($r^2 = 0.72$; $n = 152$). Importantly, data collected during 1990 coincided with the declining phase of a spring bloom. Surface (20 m) values of α^b decreased during the 1990 study in consort with diminishing NO_3^- concentrations (their fig. 1B), indicating an important role of nutrients in E_k -independent variability. Despite complications in interpretation arising from depth-dependent changes in photoacclimation, further evidence for a role of nutrients was provided by the coincidence of the nutricline with increases in α^b and P_{\max}^b at depth in stratified water columns. Platt et al. (1992) stated that parallel changes in α^b and P_{\max}^b were not due to changes in \bar{a}^* (in agreement with our OliPac results) but rather reflected variations in the quantum yield of photosynthesis (Φ).

Perhaps the most impressive display of E_k -independent variability was provided by the > 800 PE experiments conducted in Antarctic waters near Palmer Station between 1991 to 1994 (Claustre et al. 1997, Moline et al. 1998). For this data set, P_{\max}^b varied from 0.04 to $13.6 \text{ mg C} \cdot (\text{mg chl} \cdot \text{h})^{-1}$, whereas α^b ranged from 0.0004 to $0.25 \text{ mg C} \cdot \text{m}^2 \cdot \text{s} \cdot (\text{mg chl} \cdot \text{h} \cdot \mu\text{mol quanta})^{-1}$ (i.e. a factor of > 500 variability). Despite diverse sampling conditions (temperatures from -1.2 to 2°C , surface daily PAR from < 5 to $> 60 \text{ open quanta} \cdot \text{m}^{-2}$, fresh melt water to saline seawater, open water to ice-covered water, surface to subsurface), E_k was relatively constrained at an average of $77 \mu\text{mol quanta} \cdot \text{m}^{-2} \cdot \text{s}^{-1}$ ($\text{SD} = 53 \mu\text{mol quanta} \cdot \text{m}^{-2} \cdot \text{s}^{-1}$). Accordingly, α^b and P_{\max}^b were well correlated ($r^2 = 0.50$) throughout the 4-year study period (Fig. 3H). Claustre et al. (1997) suggested that changes in species composition were largely responsible for the tremendous E_k -independent variability observed but did not quantitatively demonstrate such a dependence.

To the best of our knowledge, the studies thus described represent all the field-based publications specifically addressing positive correlations in α^b and P_{\max}^b . Unquestionably, similar relationships exist in many historical data sets but have simply gone overlooked. None of these studies demonstrates a physiological basis for E_k -independent variability, but some have identified variables that apparently do not contribute significantly (e.g. \bar{a}^* , surface PAR, temperature). These field data also document that α^b is far from constant and can vary, along with P_{\max}^b , by over 2 orders of magnitude (Fig. 3). An evaluation of potentially important metabolic pathways and our proposed mechanism for E_k -independent variability will follow shortly, but first in the next section we review the relevant laboratory studies.

DIEL CYCLES IN LABORATORY MONOCULTURES: AN EQUIVALENT PHENOMENON?

Covariations in α^b and P_{\max}^b are most commonly (but not exclusively) observed in the laboratory during

studies on diel periodicity. Assuming equivalent underlying mechanisms, these controlled experiments may provide some insights on the physiological nature of the oscillations observed in the field at similar to interannual time scales. In the laboratory, daily photosynthetic rhythms have been extensively studied since the pioneering work of Sorokin in the 1950s, and detailed reviews can be found in Harding et al. (1981a) and Prézélin (1992). Here, we focus only on those studies reporting biomass-independent parallel changes in α and P_{\max} .

Available data suggest that daily rhythms in photosynthesis occur in all major taxonomic groups of phytoplankton. For prokaryotic algae, parallel changes in α^b and P_{\max}^b (measured as ^{14}C uptake) have been documented in light–dark-synchronized cultures of marine *Synechococcus* (Prézélin 1992) and *Prochlorococcus* (F. Bruyant, unpublished observations), with both variables fluctuating by more than 2-fold in the former species and 4-fold in the latter (see PROMOLEC: AN EXAMPLE FROM THE LABORATORY, below). In eukaryotic algae, significant diel periodicity in α^b and P_{\max}^b (measured as ^{14}C uptake or O_2 production) has been confirmed in multiple marine diatom, dinoflagellate, chlorophyte, and chrysophyte species (Harding et al. 1981a) and in the freshwater chlorophytes, *Acetabularia* (Terborgh and McLeod 1967), *Chlamydomonas*, *Chlorella*, and *Scenedesmus* (Sorokin and Krauss 1961, Senger and Bishop 1967, Senger 1970a, b, 1975). The degree of variability appears particularly pronounced in diatoms, with some species exhibiting a 20-fold or greater change over a diel cycle (Harding et al. 1981a,b).

In addition to species-dependent differences, the amplitude of diel photosynthetic oscillations appears to vary with growth rate, dampening with increased nutrient or light limitation but persisting at a low level even during stationary phase (Harding et al. 1981b, 1982, 1987, Post et al. 1985, Putt and Prézélin 1988, Prézélin 1992). The timing of diel rhythms relative to the light–dark cycle appears reasonably conserved, with α^b and P_{\max}^b generally beginning to increase during the final hours of the night, peaking in the morning or near noon, and then reaching a minimum late in the photoperiod or early in the evening (Prézélin and Sweeney 1977, Putt and Prézélin 1988, Prézélin 1992, Bruyant et al. in prep). Neither light nor the cell division cycle, however, appears to directly control the diel changes in α^b and P_{\max}^b , because oscillations can persist for several cycles after transfer to constant light (Hastings et al. 1961, Prézélin and Sweeney 1977, Harding et al. 1981a) or darkness (Hellebust and Terborgh 1967) and are observed in slow-growing and nutrient-limited algae with division rates $< 1 \text{ d}^{-1}$ (Prézélin 1992).

Despite its common occurrence, there are several reports where no parallel periodic changes in α^b and P_{\max}^b were observed in cultures grown under light–dark cycles. Several explanations are possible. For example, diel covariance may not exist in some species, such as in

macroalgae that exhibit large diel oscillations in P_{\max}^b but not α^b (Mishkind et al. 1979, Henley et al. 1991, Henley 1993). The lack of diel periodicity in α^b and P_{\max}^b could also result from rapid growth. Specifically, Harding et al. (1981a) observed no diel photosynthetic rhythms in *Pheodactylum tricornutum*, *Skeletonema costatum*, and *Dunaliella tertiolecta* when specific growth rates (μ) greatly exceeded 0.69, but clear diel cycles were observed in the same species when $\mu \sim 0.69$ (i.e. one division per day). Photosynthetic periodicity can also be missed simply because of inadequate sampling. Because the rate of diel changes in α^b and P_{\max}^b is quite high (Harding et al. 1981a), proper characterization of the cycle amplitude and timing requires reasonably high sampling frequencies ($\leq 2 \text{ h}$). Finally, some studies might suffer from technical difficulties in precise determination of α^b .

Physiology of the diel oscillations. There has been no consensus on the underlying mechanism or combination of mechanisms responsible for observed diel changes in P_{\max}^b or the covariance between α^b and P_{\max}^b . However, the general understanding is that the diel rhythms result from feedback metabolic oscillations caused by growth under nonsteady environmental conditions. Important environmental perturbations include periodicity in light (day–night cycles, diurnal changes in irradiance) and exogenous nutrient supply, which in turn synchronize cell division and set intrinsic endogenous rhythms (internal clocks). According to Post et al. (1985), diel modulation of photosynthesis reflects changes in energy and carbon requirements during each phase of the cell cycle. High photosynthetic activities support periods of accelerated biopolymer synthesis and growth (Post et al. 1985), whereas biomass build-up, nutrient uptake, and light utilization are down-regulated during cell division (Raateoja and Seppala 2001). The observation that the intensity of growth irradiance has only a minor effect on the timing of the diel cycle (Raateoja and Seppala 2001) suggests that the signal for feedback regulation is related to the fulfillment of metabolic requirements for cell division.

Suggested regulatory targets involved in diel photosynthetic rhythms have included both electron transport processes of the thylakoid membrane and downstream metabolic pathways. Prézélin and Sweeney (1977) favored the former, noting that equivalent changes in α^b and P_{\max}^b seem to exclude the possibility of regulation at the level of enzyme concentration or activity. Hellebust et al. (1967) accordingly found no relationship between photosynthetic performance and the activity of reductive pentose cycle enzymes in *Acetabularia*. Senger and Bishop (1967) and Senger (1975) concluded that parallel changes in α^b and P_{\max}^b in *Scenedesmus* were largely driven by changes in PSII activity, with minimal changes of PSI. Likewise, Samuelsson et al. (1983) found that PSII activity (measured as Hill reaction rates in isolated thylakoids) accounted for diel changes in photosynthesis in *Gonyaulax*, whereas PSI activity showed no periodicity.

Kaftan et al. (1999) proposed that decreases in photosynthetic activity in *Scenedesmus* at the end of the light period resulted from an accumulation of inactive PSII centers that could not be repaired due to cell cycle-related rearrangements of the thylakoid membranes. Prézélin and Sweeney (1977) similarly suggested that diel photosynthetic cycles resulted from changes in the fraction of active photosynthetic units. However, the lack of concomitant changes in the apparent size of photosynthetic units (chl/O₂) (Schmid and Gafron 1968, Myers and Graham 1975) and evidence that photosynthesis is limited downstream of PSII at light saturation (Kok 1956, Sukenik et al. 1987, Behrenfeld et al. 1998) are not consistent with variability in PSII activity being the central mechanism for parallel changes in α^b and P_{\max}^b . Alternative proposals of thylakoid-related mechanisms have included changes in the concentration of active cytochrome *b₆f* complexes (Wilhelm and Wild 1984), and membrane feedback involving the coupling/uncoupling of whole photosynthetic units as a result of ion fluxes (K⁺) across the thylakoid membrane (Herman and Sweeney 1975, Adamich et al. 1976, Prézélin and Sweeney 1977, Sweeney et al. 1979).

Other evidence locates the site of regulation outside of the thylakoid membranes. Loneragan and Sargent (1979) found that changes in photosynthesis were not associated with oscillations in PSII or PSI activities in *Euglena*. Myers and Graham (1975) observed that changes in P_{\max}^b in synchronous cultures of *Scenedesmus* were accompanied by changes in the turnover rate, but not size, of the photosynthetic units and concluded that regulation of downstream metabolic machinery was far greater than that of photosynthetic machinery. Analysis of diel photosynthetic cycles in the macroalga, *Ulva*, indicated that endogenous circadian rhythms modulate the activity of the carbon fixation reactions (Mishkind et al. 1979). Carbon concentrating mechanisms may also play a role in regulating photosynthetic performance. For example, in cultures of *Chlamydomonas* synchronized by a light-dark cycle and grown at low CO₂, the period of maximal photosynthetic activity coincided with increased affinity for extracellular C, increased activity of carbonic anhydrase, and increased intracellular CO₂ concentration (Marcus et al. 1986). Similarly, peak photosynthetic rates (measured as O₂ evolution) and carbonic anhydrase activities were coincident in synchronized cultures of *Chlorella ellipsoidea* (Nara et al. 1989).

Finally, although no direct link has been made between nitrogen assimilation and the parallel diel changes in α^b and P_{\max}^b , we note here that several laboratory studies have shown that nutrient (NO₃⁻ or NH₄⁺) assimilation is highest in the early phase of the light cycle (Gao et al. 1992, Berges et al. 1995, Vergara et al. 1998), which coincides with the time of highest carbon fixation activity. In *Thalassiosira*, the level of expression of nitrate reductase is correlated with the integrated pool of organic carbon accumulated during the preceding photoperiod and enhanced nitrate

reductase activity begins *before* the end of the dark period (Vergara et al. 1998).

Neither the field studies nor laboratory studies thus described have yielded a consistent physiological explanation for E_k-independent variability, although some dependencies have been identified and its prevalence over wide spatial (single cells to populations) and temporal scales (hours to years) has been documented. In the following sections, we investigate further the potential mechanisms by which positive correlations in α^b and P_{\max}^b may emerge. We start by analyzing the basic equations describing electron transport through PSII and later consider metabolic pathways downstream of PSII.

COMMON DEPENDENCIES OF α^b AND P_{\max}^b AT THE LEVEL OF BASIC PHOTOCHEMISTRY

The potential for significant variations in photosynthetic yields is very much dependent on the "currency" being considered. The quantum efficiency for electron transfer from water to the acceptor side of PSII is far more constrained than that of net O₂ evolution, which likewise is more constrained than the quantum efficiency for carbon fixation. These differences reflect the ever increasing number of alternative pathways for electron flow between the initial charge separation reactions and the consummate creation of organic material. In this section, we consider photosynthesis simply as the photochemical reactions around PSII that result in electron transfer from water to the plastoquinone (PQ) pool. From this perspective, we look to the basic equations for electron transfer to identify shared variables that can potentially account for the positive correlations in light-limited and light-saturated photosynthesis.

At the level of PSII photochemistry, the light-limited slope (α_{PSII}) is the product of the number of PSII reaction centers in a sample volume (n_{PSII}), the fraction of those PSII centers that are photochemically competent (f_{PSII}), and the average functional absorption cross-section of the competent centers (σ_{PSII}):

$$\alpha_{\text{PSII}} = n_{\text{PSII}} \times f_{\text{PSII}} \times \sigma_{\text{PSII}} \quad (1)$$

Equation 1 neglects charge recombination or cyclic electron flow around PSII, because these processes generally represent negligible electron flow at low light (Prasil et al. 1996).

In similar terms, chl concentration can be expressed as a function of n_{PSII} , the chl concentration per PSII ($\text{chl}/_{\text{PSII}}$), the number of PSI reaction centers in the sample (n_{PSI}), and the chl concentration per PSI ($\text{chl}/_{\text{PSI}}$):

$$\text{chl} = (n_{\text{PSII}} \times \text{chl}/_{\text{PSII}}) + (n_{\text{PSI}} \times \text{chl}/_{\text{PSI}}) \quad (2)$$

If we assume that $\text{chl}/_{\text{PSII}}$ and $\text{chl}/_{\text{PSI}}$ are similar, then substitution and rearranging yields

$$\text{chl} = n_{\text{PSII}} \times \text{chl}/_{\text{PSII}} \times (1 + \text{PSI:PSII}) \quad (3)$$

where PSI:PSII is the number ratio of the two photosystems.

The term chl/PSII in Eq. 3 is related to the target size of PSII complexes. The product of chl/PSII and \bar{a}^* yields the *optical* absorption cross-section of PSII (\mathbf{a}_{PSII}), which is affiliated with the *functional* absorption cross-section (σ_{PSII}) through the photochemical efficiency for absorbed quanta (Φ_p):

$$\sigma_{\text{PSII}} = \mathbf{a}_{\text{PSII}} \times \Phi_p = \text{chl}/\text{PSII} \times \Phi_p \times \bar{a}^* \quad (4)$$

At the level of PSII, there are only three potential fates for absorbed photons: charge separation, fluorescence, or thermal dissipation. Φ_p simply represents the fraction of photons absorbed by functional PSII complexes that result in primary charge separation, as opposed to fluorescence (Φ_f) or heat (Φ_H) loss. It is still unclear from laboratory and field studies how photons absorbed by nonfunctional PSII centers influence either Φ_p or σ_{PSII} .

Combining Eqs. 1, 3, and 4 gives the chl-normalized light-limited slope for electron transport from water to the PQ pool (α_{PSII}^b):

$$\alpha_{\text{PSII}}^b = f_{\text{PSII}} \times \Phi_p \times \bar{a}^* \times (1 + \text{PSI:PSII})^{-1} \quad (5)$$

Note in Eq. 5 that normalizing α to chl removes any explicit dependence of the light-limited slope on n_{PSII} and σ_{PSII} . With respect to E_k -independent variability in PE curves, we have already discussed that changes in \bar{a}^* do not appear to contribute significantly. Thus, if the positive correlation between α^b and P_{max}^b is rooted in basic photochemical processes around PSII, then it must be associated with one or more of the remaining three variables in Eq. 5, namely f_{PSII} , Φ_p , and PSI:PSII (note that deviations from our assumption of $\text{chl}/\text{PSII} = \text{chl}/\text{PSI}$ will also contribute to α_{PSII}^b variability).

Potential flexibility in α_{PSII}^b can be qualitatively evaluated by considering the potential range of independent variability in the three critical variables of Eq. 5. First, if the ratio of variable to initial fluorescence (F_v/F_0) is taken as a measure of photochemically competent PSII centers (Crofts et al. 1993), then a reasonable range for f_{PSII} in phytoplankton is ~ 0.3 to 1.0 (Behrenfeld et al. 1998, 1999) (note that $F_v/F_0 = F_v/F_m / (1 - F_v/F_m)$). Next, laboratory studies suggest that PSI:PSII ratios vary between ~ 0.2 and 3.0 over a very wide range of growth conditions (Malkin and Niyogi 2000), although the diversity of species represented by these studies is limited. Finally, changes in Φ_H have the potential to cause large changes in Φ_p (note that $\Phi_p + \Phi_f + \Phi_H = 1$), but the extent to which Φ_H varies in functional PSII complexes is not well understood and is likely taxonomically dependent. In addition, the relatively long-term incubations associated with practical PE determination minimize the influence of rapidly reversed Φ_H processes on α^b . The constraints thus considered are precisely the same constraints that have constituted the historical basis for treating α^b as essentially constant.

Identifying sources of variability in light-saturated electron transfer from water to the PQ pool ($P_{\text{m-PSII}}$) is dependent on whether rate limitation is at or down-

stream of PSII. In the former case, electron turnover potential for the ensemble of PSII complexes is

$$P_{\text{m-PSII}} = n_{\text{PSII}} \times f_{\text{PSII}} \times 1/\tau_{\text{PSII}}^* \quad (6)$$

where τ_{PSII}^* is the maximum turnover rate per functional PSII (Behrenfeld et al. 1998). Equations 3 and 6 can be combined to give the chl-normalized light-saturated rate ($P_{\text{m-PSII}}^b$):

$$P_{\text{m-PSII}}^b = f_{\text{PSII}} \times [\text{chl}/\text{PSII} \times \tau_{\text{PSII}}^* \times (1 + \text{PSI:PSII})]^{-1} \quad (7)$$

Comparison of Eqs. 5 and 7 indicates that only f_{PSII} and PSI:PSII are common to expressions for α_{PSII}^b and $P_{\text{m-PSII}}^b$ and thus can potentially contribute to E_k -independent variability.

Evidence that P_{max} is limited downstream of PSII under most growth conditions is overwhelming (Kok 1956, Weinbaum et al. 1979, Björkman 1981, Wilhelm and Wild 1984, Sukenik et al. 1987, Heber et al. 1988, Leverenz et al. 1990, Rivkin 1990, Orellana and Perry 1992, Behrenfeld et al. 1998, Geider and McIntyre 2002). Thus, the appropriate expression for $P_{\text{m-PSII}}$ is

$$P_{\text{m-PSII}} = n_{\text{LF}} \times 1/\tau_{\text{LF}} \quad (8)$$

where n_{LF} is the concentration of the rate-limiting photosynthetic component (e.g. *cyt b₆f*, RUBISCO, PQ molecules, etc.) and $1/\tau_{\text{LF}}$ is the maximum turnover rate of this component. Normalization of $P_{\text{m-PSII}}$ to chl (Eq. 3) yields

$$P_{\text{m-PSII}}^b = n_{\text{LF}} \times [n_{\text{PSII}} \times \text{chl}/\text{PSII} \times \tau_{\text{LF}} \times (1 + \text{PSI:PSII})]^{-1} \quad (9)$$

Comparison of Eqs. 5 and 9 now indicates that only the PSI:PSII ratio links α_{PSII}^b and $P_{\text{m-PSII}}^b$ at the level of basic photochemistry (assuming $\text{chl}/\text{PSII} \approx \text{chl}/\text{PSI}$). Given the restricted range in PSI:PSII ratios observed in the laboratory, it would appear that the potential for significant positive correlations in α^b and P_{max}^b to result from variability in the initial light reactions of photosynthesis is small.

Our conclusion in this section is consistent with the results of Behrenfeld et al. (1998). In that study, changes in α^b and P_{max}^b in *Thalassiosira weissflogii* were followed as functional PSII complexes were progressively blocked by titration with 3-(3,4-dichlorophenyl)-1,1-dimethylurea. Their results indicated that 1) changes in PSII functioning resulted in covariations in α^b and P_{max}^b only under growth conditions resulting in the limitation of light-saturated electron transport by PSII (e.g. when cells were acclimated to very high light [$1000 \mu\text{mol quanta} \cdot \text{m}^{-2} \cdot \text{s}^{-1}$]) and that 2) under such conditions, P_{max}^b varied in proportion to f_{PSII} . The general insensitivity of P_{max}^b to changes in f_{PSII} has been demonstrated for a variety of growth conditions (Kok 1956, Weinbaum et al. 1979, Heber et al. 1988, Leverenz et al. 1990). Collectively, these results indicate that we should look toward processes downstream (i.e. on the acceptor side) of PSII to find the

more common underlying mechanism for observed positive correlations in α^b and P_{\max}^b .

LIFE AFTER PSII: DOWNSTREAM METABOLIC PATHWAYS

The two basic means by which downstream pathways influence PE variables are by diverting electrons to noncarbon sinks (e.g. nitrogen reduction) and by transferring electrons back to O_2 on a time scale significantly shorter than the PE measurement. For covariations in α^b and P_{\max}^b to result, the *fraction* of photosynthetic product (i.e. reductant) allocated to these alternative pathways must be independent of light, with the former process influencing carbon fixation only and the latter altering both carbon fixation and oxygen evolution. In this section, we begin by tracing electron transport from PSII to the primary cell reductants and then evaluate alternative pathways for these reductants in terms of their potential to cause significant parallel changes in α^b and P_{\max}^b .

From PSII to reductants. Starting from PSII, electrons are transferred to an intermembrane PQ pool, a membrane-bound cytochrome complex (cyt $b_6 f$), a mobile cytochrome (cyt c_{553}) or plastocyanin, PSI, and then rapidly through a series of carriers (a monomeric chl a , phylloquinone, and iron-sulfur centers F_X , F_A , F_B) to ferredoxin (Fig. 4A). During this electron transport sequence, protons (H^+) are transferred across the thylakoid membrane to the lumen to create a proton motive force that drives ATP synthesis via the membrane-bound ATP synthase complex (~ 1 ATP per 4 H^+ translocated) (Fig. 4A). In eukaryotic photoautotrophs, little opportunity exists between PSII and ferredoxin for recombination of electrons with O_2 , whereas in prokaryotes significant electron flow from PSII to O_2 before PSI can occur because of the collocation of photosynthetic and respiratory electron transport components (Scherer 1990). As detailed later, we suggest that this alternative pathway (and its analogue in eukaryotes) plays a central role in α^b and P_{\max}^b covariations.

Although often considered an intermediate product of PSI oxidation, reduced ferredoxin (or flavodoxin in the case of iron-limiting conditions) represents a significant branching point for a variety of pathways, including reduction of thioredoxin, the Mehler reaction, nitrogen assimilation, and $NADP^+$ reduction (Noctor and Foyer 2000). Thioredoxin represents too minor an electron sink to directly cause α^b and P_{\max}^b to covary, but it can play a critical role in the light-dependent regulation of photosynthate allocation (Malkin and Niyogi 2000, Geider and MacIntyre 2002). The Mehler reaction is also unlikely to be responsible for significant parallel changes in α^b and P_{\max}^b , because it is largely restricted to light-saturating conditions (Kana 1992, Ort and Baker 2002). This “pseudocyclic” pathway transfers electrons from ferredoxin back to O_2 (Fig. 4A), but it involves potentially damaging reactive intermediates (superoxide, H_2O_2) and is thus inhibited when substrates for alternative

pathways are available (e.g. $NADP^+$, NO_3^- , or oxaloacetate [OAA]) (Noctor and Foyer 2000). The Mehler reaction results in ATP synthesis without net reductant production and is thought to play a protective role at very high light levels when the demand for ATP is high relative to reductant (Egneus et al. 1975).

When substrate is available, the preferred pathway from ferredoxin is the transfer of two electrons and two H^+ to $NADP^+$, forming NADPH (Fig. 4A). NADPH is central to a variety of metabolic pathways, including Calvin-Benson cycle carbon fixation, and can be used equally with ferredoxin in the nitrogen reduction pathway. NADPH can also readily reduce NAD^+ to form NADH, and *visa versa*. Together, NADPH, NADH, and ferredoxin represent the primary reductants for cell metabolism. Concurrent *trans*-membrane H^+ transfer during photosynthesis results in a production ratio of ~ 1.5 ATP:NADPH in eukaryotic algae, although changes in membrane permeability to H^+ , the H^+ :ATP yield of ATP synthase, and cyclic H^+ pumping at cyt $b_6 f$ (the “Q cycle”) or around PSI do permit a limited degree of variability in this ratio within the chloroplast (Noctor and Foyer 2000).

Spending the photosynthetic currency. The light-harvesting and electron transport sequence generates, in relatively constrained proportions, the “currency” of metabolism: ATP and simple reductants. This currency is spent in pathways such as carbon fixation, nitrogen assimilation, photorespiration, inorganic carbon accumulation, chlororespiration, pseudocyclic electron transport (e.g. Mehler reaction), and respiratory phosphorylation (i.e. oxidation of NAD(P)H to create ATP) (Fig. 4). Each of these pathways influences ATP and reductant pools differently. The prominence of any particular pathway is dependent on the temporal separation of metabolic events (Li et al. 1980, Cuhel et al. 1984) and on the balance between maintenance (high ATP, low reductant demand) and growth (high reductant demand). A suite of regulatory mechanisms has evolved to ensure stability in the redox states of adenylate and reductant pools despite highly variable supply and demand. The efficacy of this regulatory system is particularly impressive when the small size and rapid turnover rates (< 1 s) of the pools are considered (Noctor and Foyer 2000).

Carbon fixation by the Calvin-Benson cycle supplies glyceraldehyde 3-phosphate (GAP) to rapid turnover (e.g. amino acid biosynthesis) and storage pathways (e.g. carbohydrate synthesis) (Fig. 4B). The ATP:reductant requirement for the Calvin-Benson cycle is 1.5, which nicely matches the photosynthetic production ratio. The fraction of photosynthate allocated to carbon fixation changes with growth conditions and on time scales from seconds to generations. Sophisticated regulatory mechanisms coordinate carbon fixation with other metabolic pathways. One of the primary regulatory steps is the carboxylation of ribulose-1,5 bisphosphate (RuBP) by the obligatory enzyme, RUBISCO. Coarse regulation of this step is achieved by

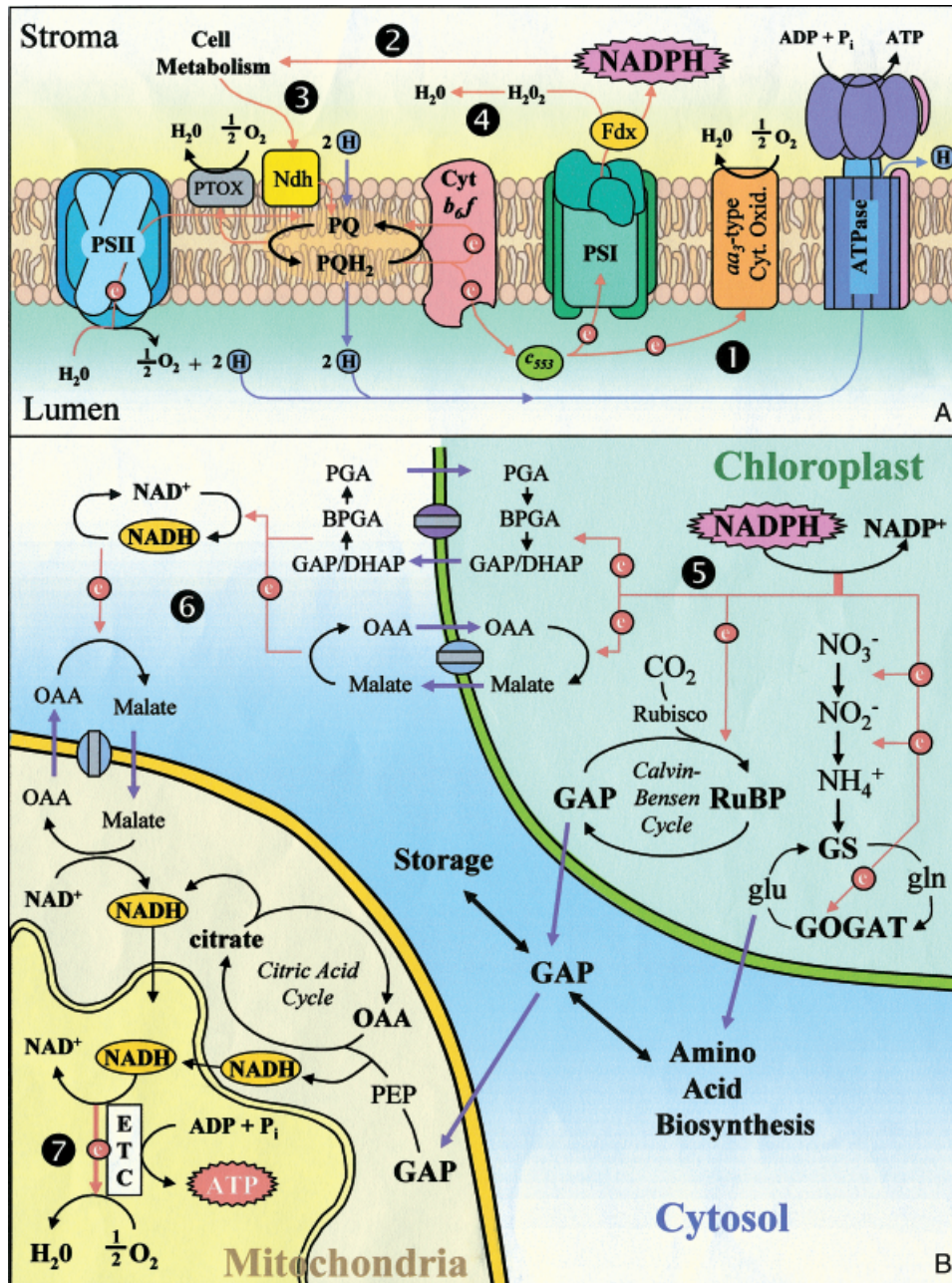


FIG. 4. Photosynthetic and metabolic electron transport pathways. (A) A "cyanobacterial-type" thylakoid membrane. Light absorption by PSII results in oxygen production and electron transport (red arrows) from water to the plastoquinone pool (PQ → PQH₂). With potentially some cycling around cytochrome *b₆f*, electrons are passed to cytochrome *c₅₅₃* and then can either continue through to PSI, ferredoxin (Fdx), and NADP⁺ to produce the reductant, NADPH, or they can be transferred through a membrane-bound oxidase (*aa₃*-type cytochrome) back to oxygen. This latter pathway (1) to oxygen is proposed here to play a critical role in the expression of E_k-independent variability in prokaryotes. Its corollary in eukaryotes is shown in B as the sequence (5-6-7). In the light, NADPH is used in a variety of downstream metabolic pathways (2), with some of the resultant products leading back to the PQ pool at night in prokaryotes (3). At very high light, electrons may also pass from Fdx back to water via the Mehler reaction (4). Pathways 1 through 4 result in a transmembrane proton gradient that is used to generate ATP by proton (H) transport from the lumen to the stroma via the ATPase complex. (B) Downstream metabolic pathways from NADPH include nitrogen reduction and glutamate (glu) synthesis via the GS-GOGAT cycle, carbon reduction and triose phosphate (GAP) export, and ATP synthesis through oxygen reduction (7) via the mitochondrial electron transport chain (ETC) and substrate shuttles (6) linking the chloroplast, cytosol, and mitochondria. The two shuttles shown here are the oxaloacetate-malate (OAA-Malate) and dihydroxyacetone phosphate-phosphoglycerate (DHAP-PGA) shuttles. GAP produced by the Calvin-Benson cycle can be used for long-term carbon storage (which is generally a one-way path in the light), carbon skeletons for amino acid biosynthesis, or mitochondrial ATP synthesis via the citric acid cycle. Electron pathways illustrated in A and B are not comprehensive and have neglected multiple alternatives, including cyclic electron flow around PSII and PSI, photorespiration, and metabolic pathways common to multiple cellular compartments (e.g. carbohydrate formation). Purple arrows, transport across membranes; Ndh, prokaryotic dehydrogenase complex; PTOX, stromal terminal oxidase; RuBP, ribulose-1, 5 biphosphate; gln, glutamine; PEP, phosphoenolpyruvate; BPGA, glycerate-1, 3-bisphosphate. Membrane-imbedded ovals with gray bar indicate decarboxylate translocators for the OAA-Malate shuttle and a phosphate translocator for the DHAP-PGA shuttle.

varying RUBISCO concentration at time scales on the order of cell division (Björkman 1981, Sukenik et al. 1987, Rivkin 1990, Orellana and Perry 1992), whereas finer and shorter time-scale adjustments are accomplished through changes in enzyme activity (Geider and MacIntyre 2002). The importance of this latter regulation is evidenced by the wide range of mechanisms involved, including 1) “sink limitation” by RuBP availability, 2) binding of sugars in the active site or binding of RuBP without CO₂ and Mg²⁺ (required for catalytic competence), 3) binding of effectors (e.g. sulfate, phosphate, RuBP) at sites other than the active site, 4) ADP:ATP-dependent changes in the thioredoxin pathway for RUBISCO activase production, and 5) CO₂ limitation resulting in enhanced oxygenase activity (photorespiration) (Geider and MacIntyre 2002). A tremendous capacity for rapid (seconds) feedback control of electron flow through the Calvin-Benson cycle, without concurrent changes in enzyme concentration, has been demonstrated by nitrogen-pulse experiments (Elrifi and Turpin 1986, 1987, Elrifi et al. 1988, Turpin 1991). With respect to observed covariations of α^b and P_{\max}^b , this up- and down-regulation of carbon reduction assists in the flexible diversion of reductants among alternative pathways.

In addition to controls on the activity of the Calvin-Benson cycle, another highly relevant aspect of carbon metabolism is the directional regulation of electron flow. The Calvin-Benson cycle and the glycolytic pathway share a variety of enzymes (e.g. aldolase, transketolase, glyceraldehyde 3-phosphate dehydrogenase) that are collocated in the cell and catalyze reversible reactions. It is therefore critical that the synthetic mode of these enzymes be “on” and the degradative mode be “off” in the light to prevent futile cycling (Siedow and Day 2000). This regulation is accomplished through a variety of means (only some of which are understood), including light-dependent H⁺ gradient effects on the pH and Mg²⁺ activation of stromal enzymes and the activation/deactivation of multiple enzymes by thioredoxin (Siedow and Day 2000). In a similar manner, down-regulation of the tricarboxylic acid cycle also occurs in the light, with a primary regulatory target being the pyruvate dehydrogenase enzyme complex. Like RUBISCO, pyruvate dehydrogenase enzyme complex is regulated in a complex manner, including activation by a protein kinase and ATP-dependent phosphorylation and deactivation by NH₄⁺, a build-up of acetyl-CoA, and high NADH concentrations (Siedow and Day 2000). Arresting storage carbohydrate catabolism and limiting tricarboxylic acid cycle activity in the light (Weger et al. 1989), however, presents a significant problem: An important ATP source is lost. As detailed shortly, balancing the supply of ATP and reductant in the light with cellular demands is achieved, in part, through rapid pathways from simple photosynthetic reductants back to O₂.

Photorespiration is one of the alternative pathways for photosynthetic reductants. Photorespiration is initiated by the oxygenase activity of RUBISCO and

results in the consumption of RuBP to form GAP and the two-carbon sugar, phosphoglycolate (Osmond 1981). Photorespiration can influence ATP:reductant ratios through extracellular excretion of phosphoglycolate or complete oxidation of phosphoglycolate to the terminal acceptor, O₂ (reductant losses) (Geider and MacIntyre 2002). Degradation of the RuBP pool, however, leads to “sink limitation” of this pathway and limits its potential for causing significant covariations in α^b and P_{\max}^b . In addition, active carbon accumulation suppresses photorespiration in most algal species by decreasing RUBISCO oxygenase activity (Birmingham et al. 1982, Weger et al. 1989). Notably, inorganic carbon accumulation requires high amounts of ATP (Noctor and Foyer 2000) and shifts overall ATP:reductant demands to > 1.5 in the light when glycolysis is minimal.

In addition to carbon products, algal growth requires reduced nitrogen. If based on NO₃⁻, assimilation to an α -amino acid (e.g. glutamate) requires 10 electrons and 1 ATP (Fig. 4B). From glutamate, biosynthesis of other amino acids requires provision of carbon skeletons, initially in the form of GAP, and is associated with stimulated respiratory CO₂ release in the light (Birch et al. 1986, Weger et al. 1988, Weger and Turpin 1989). Diversion of electrons from carbon fixation to nitrogen reduction can cause parallel changes in carbon-based, but not oxygen-based, α^b and P_{\max}^b . The enhanced respiration associated with amino acid biosynthesis, however, can alter both oxygen- and carbon-based PE variables in a manner dependent on the source (new or stored) of GAP and the time scale of the measurement.

Chlororespiration is another potential rapid pathway in eukaryotic photoautotrophs for generating ATP in the light at the expense of reductants (NADH, possibly NADPH) (Bennoun 1982). Chlororespiration creates an H⁺ gradient across the thylakoid membrane via transfer of electrons from NAD(P)H, through a dehydrogenase complex (Ndh), to the PQ pool, and then to O₂ via a terminal oxidase (PTOX) (Fig. 4A). The involvement of the PQ pool in this pathway necessitates a competitive interaction with photosynthetic electron flow from PSII, which influences fluorescence characteristics accordingly. Chlororespiration is thought to represent a minimal reductant sink, particularly in the light (Peltier and Cournac 2002), and thus is an unlikely candidate for causing significant covariations in α^b and P_{\max}^b .

As alluded to earlier, it appears that a likely pathway for generating significant additional ATP in the light at the expense of reductant is to bypass the carbon fixation steps altogether and simply feed the photosynthetically generated reductants directly through the standard respiratory electron transport sequence to O₂. This pathway is shortest in prokaryotic algae because of the partial sharing of photosynthetic and respiratory machinery (Scherer 1990). In prokaryotes, electrons from PSII, ferredoxin, or NADPH are transferred through the PQ pool, to cyt *b₆f*, and then

to mobile cyt c_{553} . Respiration then involves the oxidation of cyt c_{553} by O_2 via a membrane-bound cytochrome aa_3 -type terminal oxidase (analogous to the mammalian mitochondrial terminal oxidase) (Alpes et al. 1989) (Fig. 4A). Regulation of electron transfer from cyt c_{553} to either PSI or cyt aa_3 is not well understood. Interestingly, it appears that in *Anabaena* the partial saturation constant (K_m) for these two reactions is approximately equal, leading to the suggestion that greater electron transfer to PSI in the light simply results from its order-of-magnitude faster turnover (Scherer 1990). Accordingly, electron transfer to cyt aa_3 will be enhanced if PSI turnover is restricted by, for example, exposure to darkness or substrate limitation on the acceptor side of PSI (e.g. decreased reductant requirements for biosynthesis).

In eukaryotes, separation of photosynthesis and respiration by NAD(P)H-impermeable membranes of the chloroplast and mitochondria slightly complicates the situation. However, this problem is shared with carbohydrate metabolism in the cytosol and is solved in a “bucket brigade” fashion using “substrate shuttles” (Heber 1974, Heldt et al. 1990, Raghavendra et al. 1994, Hoefnagel et al. 1998). Two prominent shuttle systems linking chloroplastic, cytosolic, and mitochondrial reductant pools are the “OAA-malate shuttle” and the “dihydroxyacetone phosphate-phosphoglyceric acid shuttle” (DHAP-PGA). The former shuttle involves the reduction of OAA to malate by NADPH in the chloroplast, subsequent transport of malate across an inner membrane in exchange for OAA, and then electron transfer from malate back to NAD(P)⁺ (Siedow and Day 2000) (Fig. 4B). The DHAP-PGA shuttle is slightly more complicated, with PGA first reduced to GAP-DHAP by NADPH through an ATP-dependent intermediate step involving glycerate-1, 3-bisphosphate, then transport of GAP-DHAP across the chloroplast membrane, and finally a reverse sequence in the cytosol to yield NADH, ATP, and PGA (Heineke et al. 1991, Raghavendra et al. 1994) (Fig. 4B). Through these shuttle systems, small completely recycled substrate pools can support extensive and rapid bidirectional transport of reductant between the chloroplast, cytosol, and mitochondria (Raghavendra et al. 1994, Gardstrom and Lernmark 1995, Hoefnagel et al. 1998). Thus, a solution for eukaryotic algae to the problem of enhanced ATP:reductant demands in the light is the cross-organelle transfer of reducing power from the chloroplast to the mitochondria for subsequent ATP formation by oxidative phosphorylation (Fig. 4B).

A PROPOSAL: DOWNSTREAM METABOLISM AND COVARIATIONS IN α^b AND P_{max}^b

From the preceding description of primary downstream electron transport pathways and their regulation, a potential explanation for covariations in α^b and P_{max}^b emerges. In addition to ATP, the basal substrate for plant metabolism provided by photosynthesis is

simple reductants, not reduced carbon compounds. Carbon fixation is only one of the potential fates for these products and its purpose is 2-fold: to provide carbon skeletons for growth and to store energy and reducing power for nocturnal metabolism. In the light, reductants formed by photosynthesis need not pass first through a reduced carbon form before complete oxidation for ATP generation. This transfer of electrons back to O_2 involves very small reductant pools with rapid turnover times and terminates almost immediately upon exposure to darkness. These characteristics prevent this pathway from being measured by standard ^{14}C - or ^{16}O -based protocols. Instead, such measurements only register reductant flow to pathways with product lifetimes similar to or longer than their experimental time scale. We propose, as a working hypothesis, that observed covariations in α^b and P_{max}^b result predominantly from changes in the fraction of reductants dedicated to fast versus longer term pathways.

The function of the fast pathway from reductant back to O_2 is to balance ATP:reductant supply with demand. One of the important characteristics of E_k -independent variability noted early on by Coté and Platt (1983) is that it is expressed over time scales ranging from hours to seasons. Accordingly, ATP:reductant demands vary over similar or even broader time scales. On shorter time scales (seconds to hours), the metabolic regulatory mechanisms, such as those described above, cause fluctuations in pathway dominance that can significantly alter ATP:reductant demands. For example, amino acid biosynthesis from newly formed GAP requires relatively large amounts of reductant for nitrogen and carbon reduction (and because recycling of CO_2 from concurrent GAP respiration minimizes ATP requirements for active inorganic carbon uptake). In contrast, higher net ATP:reductant requirements are associated with carbohydrate synthesis (partly reflecting ATP demands for inorganic carbon uptake), secondary anabolic pathways from triose- or pentose-phosphate pools to nucleic acids and structural compounds, and recycling pathways for metabolic constituents.

At the daily to seasonal scale of field measurements (Figs. 2 and 3), we propose that E_k -independent variability likewise results from changes in ATP:reductant demands, but in this case the dominant mechanism is growth rate-driven changes in pathway capacities, not regulatory enzyme activation/deactivation. Taken to an extreme, very high ATP:reductant requirements are anticipated when net growth is arrested. In such a case, the fast oxidative pathway for NADPH supplies the required ATP in the light for recycling processes that maintain metabolic constituents and only a minimum carbon fixation capacity is required to support nocturnal activity. In contrast, rapid growth requires significant reductant investments into new carbon compounds and necessitates enhanced daytime carbohydrate storage to support elevated nocturnal metabolism. This interpretation is

consistent with observations that α^b and P_{\max}^b can covary with nutrient availability (Platt et al. 1992) and can exhibit exceptional variability under the extreme growth conditions around Antarctica (Moline et al. 1998) (Fig. 3H).

PROMOLEC: AN EXAMPLE FROM THE LABORATORY

In this section, we use data from the “ProMolec” experiment, a 1999 laboratory study, to illustrate how diel patterns in α^b and P_{\max}^b can be consistent with our proposed mechanism of time-dependent changes in reductant allocation. The ProMolec study involved the oxyphotobacterium *Prochlorococcus* (strain PCC 9511) acclimated in axenic nutrient-replete cyclostats for 15 days before an extensive (every 2 h) 3-day monitoring period. Details on experimental design and methods can be found in Steglich et al. (2001) and P. Bruyant, unpublished observations. Measurements included variable fluorescence, ^{14}C -based PE relationships, divinyl chl *a* concentrations, \bar{a}^* , flow cytometry-based cell number, size, DNA content, and an analysis of transcription levels for the gene encoding the large subunit of RUBISCO (*rbcL*) (Steglich et al. 2001, P. Bruyant, unpublished observations).

During the three diel cycles monitored, α^b and P_{\max}^b exhibited exceptional variability (factor of >4) and remarkable temporal coherence ($r^2 = 0.88$) (Fig. 5A). Photosynthetic rates were low during cell division (sunset to midnight; Fig. 5B), increased rapidly after midnight along with *rbcL* expression (Fig. 5C), remained high until approximately noon, and then dropped dramatically and remained low until the end of the subsequent division cycle (Fig. 5A). During each photoperiod, the only time when cellular carbon fixation ($P^{\text{cell}} = P_{\max}^b \times \tanh(\alpha^b \times I_0 \times P_{\max}^{b-1}) \times (\text{divinyl chl } a \cdot \text{cell}^{-1})$) matched the rate of cellular carbon accumulation (ΔC) was after the midday drop in α^b and P_{\max}^b (Fig. 5D). Clearly, afternoon carbon fixation was devoted to the formation of storage products with lifetimes greater than 2 h (i.e. the sampling interval). In contrast, the large discrepancy between P^{cell} and ΔC in the morning (Fig. 5D) indicated the prominence of a carbon pathway with product lifetimes longer than 20 min (i.e. length of the ^{14}C incubations) but shorter than 2 h. Importantly, neither the near-noon drop or the overall diel pattern in carbon fixation was associated with similar changes in \bar{a}^* , cellular divinyl chl *a*, energy transfer to PSII (σ_{PSII}), or the efficiency of primary charge separation at PSII (F_v/F_m) (P. Bruyant, unpublished observations). These results strongly indicated that the measured changes in α^b and P_{\max}^b were not associated with parallel changes in photosynthetic electron transport. Instead, these diel patterns are consistent with the time-regulated diversion of reductants to alternative pathways.

Taking sunset as a starting point, we interpret the first 6 h of the diel cycle as being focused on cell division, with little need to adjust photosynthetic

potentials and having only a minor influence on N:C ratios (Fig. 5B). Dilution of cellular constituents by division, however, required subsequent synthesis of both Calvin cycle and light-harvesting components (Fig. 5C), which accordingly depleted carbon reserves and increased N:C ratios between midnight and dawn (Fig. 5B). The depletion of carbohydrate and amino acid pools poised the Calvin cycle for enhanced reductant flow at sunrise, as revealed in cells taken from the predawn darkness and exposed to light (Fig. 5A). High values of α^b and P_{\max}^b and coincident slow carbon accumulation rates (Fig. 5, A and D) indicated that instead of forming storage products, GAP production in the morning was largely dedicated to a moderate-lifetime pathway, almost certainly amino acid biosynthesis (Weger et al. 1989). This interpretation is consistent with active nitrogen reduction and amino acid biosynthesis having an inhibitory influence on carbon storage product formation (Champigny 1995, Padmasree and Raghavendra 1998).

The sharp midday decline in carbon fixation (Fig. 5A) and its sudden agreement with carbon accumulation rates (Fig. 5D) is taken as indicating a general cessation of protein synthesis, the down-regulation of Calvin-Benson cycle activity, and a shift in the remaining carbon reduction toward carbohydrate storage. The trigger for this regulatory cascade is not yet clear, but it was not associated with a corresponding change in photosynthetic electron transport (P. Bruyant, unpublished observations) or primary reductant formation. Consequently, reductant flow to the rapid oxidative pathway must have increased by a degree equal to the difference between morning and afternoon carbon fixation. This shift suggests that ATP demands also increased dramatically in the afternoon, in part likely due to enhanced net CO_2 uptake to support carbon storage product synthesis, repair of photodamaged PSII complexes, and secondary anabolic activities in preparation for cell division. The close match between carbon fixation and accumulation during this time indicated that the new ATP requirements were not being met by enhanced glycolysis and that the carbon storage products formed were not intended for daytime use.

In summary, the strong covariations in α^b and P_{\max}^b observed during ProMolec are consistent with the entrainment of *Prochlorococcus* cell division by the light-dark cycle causing a highly synchronized temporal progression in the dominance of metabolic pathways with divergent ATP and reductant requirements. In the morning, reductants were largely directed to carbon products with lifetimes long enough to be registered as net ^{14}C fixation. In the afternoon, enhanced ATP requirements resulted in the diversion of reductant away from carbon fixation (thus, not registered as ^{14}C uptake) and into a rapid oxidative pathway converting O_2 back to H_2O on a time scale of $<1\text{s}$ (i.e. in proportion to the turnover time of the reductant pools).

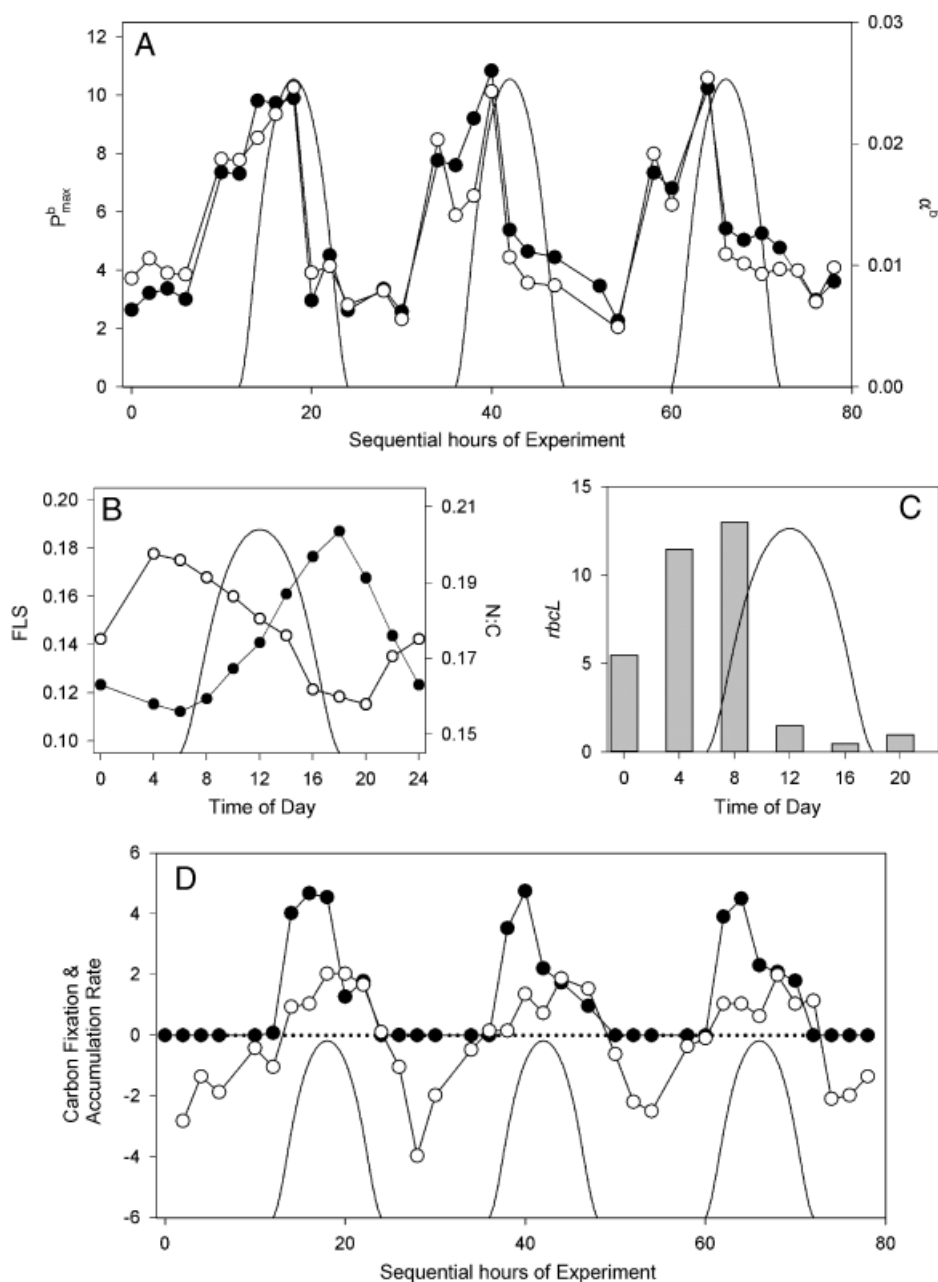


FIG. 5. Physiological variability in *Prochlorococcus* (strain PCC 9511) grown in axenic cyclostats (Bruyant et al. 2001). (A) Diel changes in the chl-normalized light-saturated rate (P_{\max}^b) and light-limited slope (α^b) of photosynthesis during three sequential photoperiods. Closed circles, P_{\max}^b ($\text{mg} \cdot \text{C} (\text{mg chl} \cdot \text{h})^{-1}$); left axis; open circles, α^b ($\text{mg C} \cdot \text{m}^{-2} \cdot \text{s} \cdot (\text{mg chl} \cdot \text{h} \cdot \mu\text{mol quanta})^{-1}$); right axis). The influence of photoinhibition on α^b has been removed using measurements of variable fluorescence and assuming α^b to change in direct proportion to F_v/F_0 (Crofts et al. 1993). (B) Average diel changes in (closed circles) relative forward light scatter (FLS) (a measure of cell size) (left axis) and (open circles) the ratio of cellular nitrogen to carbon ($\text{mg} \cdot \text{mg}^{-1}$) (right axis). (C) Average diel changes in the relative transcription level for the gene encoding the large subunit of RUBISCO (*rbcL*). (D) Time course of cellular carbon fixation (closed circles) and carbon accumulation (open circles) over three sequential diel periods. Carbon fixation was calculated from measured photosynthesis-irradiance relationships (A) and light levels using the hyperbolic tangent model of Jassby and Platt (1976) ($\text{fg C} \cdot (\text{cell} \cdot \text{h})^{-1}$). Carbon accumulation was calculated as the change in cellular carbon biomass between 2 h sampling periods ($\text{fg C} \cdot (\text{cell} \cdot \text{h})^{-1}$) and is negative during the night due to cell division and metabolism of stored carbon products. In all graphs, the sinusoidal solid line (—) indicates relative changes in incident light (range, 0–970 $\mu\text{mol quanta} \cdot \text{m}^{-2} \cdot \text{s}^{-1}$).

SUMMARY

In 1976, Platt and Jassby described striking seasonal covariations in α^b and P_{\max}^b and immediately recognized that these changes were entirely inconsistent with

contemporary dogma regarding limitations of photosynthesis at low and saturating light. In the time since, similar relationships have been repeatedly observed (Fig. 3), and in some cases quite fantastically (Fig. 3H). Diel laboratory studies have also indicated that

comparable changes in α^b and P_{\max}^b can occur within a single species over the course of only a few hours. Despite these numerous observations, the physiology of E_k -independent variability has remained elusive.

Here we attempted to take an initial step toward solving this mystery and, in doing so, have reconsidered the phenomenon's potential basis in the context of the initial reactions of photochemistry and at the broader scale of downstream metabolic processes. Our examination has led to the hypothesis that a potentially large but variable fraction of reductant formed through photochemistry is rapidly oxidized to generate ATP for metabolic processes not requiring newly formed reduced carbon products. We envision the participatory biochemical pathways as identical to those used during the final stages of carbon metabolism, namely the mitochondrial electron transport chain for oxidative phosphorylation in eukaryotes and the PQ-cytochrome *aa*₃-type pathway in prokaryotes.

One of the many important outcomes of basic plant physiological research during the past decade has been the emergent recognition of a tight coupling between chloroplast and mitochondrial metabolism in the light (Hoefnagel et al. 1998, Padmasree and Raghavendra 1998). Indeed, the critical nature of ATP generation by mitochondrial oxidative phosphorylation for optimal photosynthetic performance is no longer considered an issue of debate. Central components in this cross-organellar communication network are precisely the substrate shuttles identified in Figure 4B. Importantly, light-dependent mitochondrial ATP synthesis consumes a variable, but often large, fraction of photosynthetic reductant, is active at both limiting and saturating light levels, can play a particularly important role at low temperatures, and is thought to be influenced by nutrient stress (Hoefnagel et al. 1998, Padmasree and Raghavendra 1998). These characteristics are all consistent with the expression of E_k -independent variability reported from the field and laboratory.

Our examination has not identified a single mechanism exclusively responsible for all E_k -independent variability. For example, we described how, under certain circumstances, α^b and P_{\max}^b can covary in response to changes in PSII functionality (f_{PSII}) (Behrenfeld et al. 1998). For the more common condition where P_{\max}^b is limited downstream of PSII, we also noted a variety of electron pathways that can contribute to E_k -independent variability. However, of the pathways considered here, we concluded that the following were not *dominant* drivers of E_k -independent variability:

1. *Nitrogen reduction*—due to its influence on carbon-based, but not oxygen-based, values of α^b and P_{\max}^b ;
2. *Mehler reaction*—due to its prominence at high light but not low light;
3. *Thioredoxin reduction*—due to its minor electron requirement;

4. *Photorespiration*—due to its potential for rapid “sink limitation” and its suppression by active carbon accumulation;

5. *Chlororespiration*—due to its apparent minor role in the light and its competitive interaction with photosynthetic electron flow;

6. *Cyclic pathways around PSII and PSI*—because they do not influence downstream reductant utilization and their rates are small at low light (particularly at PSII).

We suggested that the longer time scale covariations in α^b and P_{\max}^b represented in Figure 3 result predominantly from growth-dependent changes in ATP and reductant demands. Because of their E_k -independent nature, such changes have little influence on PQ redox states at a given light level and do not interfere with photoacclimation (a PQ-redox sensitive process) (Escoubas et al. 1995, Pfannschmidt et al. 1999). This system thus enables the independent regulation of PE characteristics in response to changes in growth irradiance and nutrient supply. We recommend that such behavior be considered in future models of phytoplankton photoacclimation. In current “dynamic acclimation models” (Geider et al. 1998, Flynn 2001, Flynn et al. 2001), α^b is assumed constant and only P_{\max} varies with nutrient stress (thus, E_k changes). Consequently, an interaction is created between nutrient availability and photoacclimation that may not be realistic.

Over the history of the positive correlation issue, field observations have largely pointed toward nutrient availability and taxonomic composition as being intimately linked to covariations in α^b and P_{\max}^b . Clearly, the growth-dependent mechanism proposed here is consistent with an important role for nutrients, due to changes in growth versus maintenance demands for new reductants and variability in the energetic cost of acquiring nutrients from the environment (e.g. motility, concentrating mechanism, etc). The link between E_k -independent variability and taxonomy is not so obvious, because within the eukaryotic or prokaryotic groups the metabolic pathways are essentially identical. Nevertheless, taxonomy may play a role. At the broadest level, the shorter pathway for rapid electron transfer back to O_2 in prokaryotes (Fig. 4) may provide some resource-based advantage in low-nutrient environments (in addition to their characteristically high surface-to-volume ratios) over eukaryotes. In addition, although the basic metabolic pathways are consistent within the prokaryotic or eukaryotic lines, regulation of these pathways under differing environmental conditions does vary between species (and even ecotypes), which can yield an apparent correspondence between taxonomic composition and the expression of E_k -independent variability.

Relevance to global ocean productivity. Areal net primary production ($\text{mg C} \cdot \text{m}^{-2}$) can be calculated from plant biomass, incident solar flux, and a parameter accounting for the utilization of absorbed light energy, ϵ (Field et al. 1998, Behrenfeld et al.

2001). The PE relationship has long proven a useful construct for describing variability in algal ϵ and its response to environmental forcings. Over the global oceans, active phytoplankton pigment biomass (i.e. integrated from the surface to the 1% PAR depth) ranges from ~ 2 to $400 \cdot \text{mg chl} \cdot \text{m}^{-2}$ (Behrenfeld and Falkowski 1997). Similarly, ϵ varies by roughly two orders of magnitude. Accurate descriptions of physiological variability are thus of comparable importance to global ocean productivity estimates as water-column chl biomass, but current uncertainties in the former are far greater than the latter (Behrenfeld et al. 2002a,b).

Clearly, a robust description of algal physiology will need to accommodate both E_k -dependent and E_k -independent variability. Photoacclimation is largely responsible for E_k -dependent variability, and its characterization in surface phytoplankton populations requires information on downwelling irradiance, underwater light attenuation, and mixed layer depths (Behrenfeld et al. 2002b). We propose that E_k -independent variability can now be associated with variable growth constraints, not because of bulk changes in cellular pigmentation but rather because of shifts in the fraction of photosynthetically produced reductants allocated to net carbon fixation (Fig. 6). Developing a globally robust analytical scheme for describing E_k -independent variability will be more challenging than for photoacclimation. An alternative is to identify an

optical index of physiological variability that can be retrieved from space and then tease from this the fraction of variability due to photoacclimation versus that due to growth limitation. One obvious target for such an index is the phytoplankton chl-to-carbon ratio (Behrenfeld and Boss 2003).

PERSPECTIVE

Photosynthesis is a highly integrated and regulated metabolic process. It requires an investment of enormous resources for the creation and maintenance of the associated machinery. Accordingly, it would be naive to believe that the capacity of this machinery is anything but economically matched to the requirements of the whole cell, given its growth conditions. Our challenge is to understand what these environmental constraints are, what suite of mechanisms is available to deal with these constraints, and how these pathways are regulated in symphony with other simultaneous activities. With respect to the current problem, the greatest challenge has been to find a new “twist” in old pathways that would accommodate significant covariations in variables that have historically been considered independent.

The heterotrophic lifestyle revolves around the metabolism of reduced carbon compounds. Before embarking on this project, we had similarly perceived phototrophic life as “carbon-centric,” with products

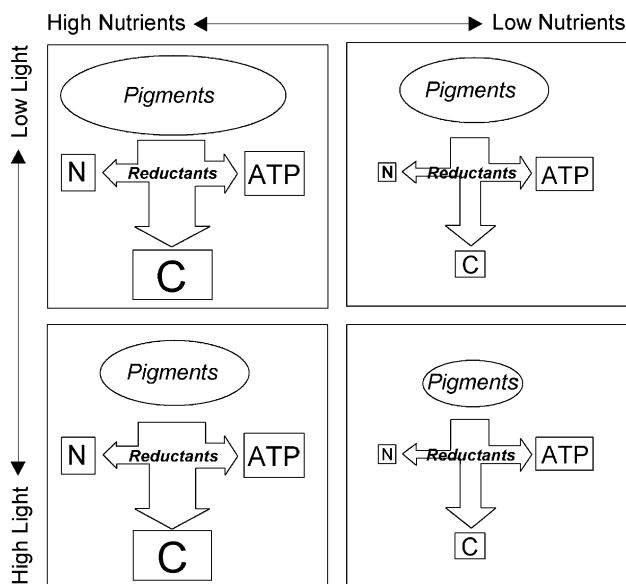
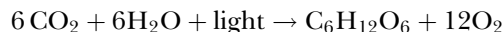


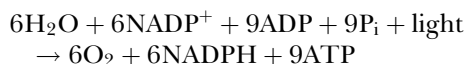
FIG. 6. Conceptualization of light and nutrient influences on pigment-specific light utilization efficiencies (ϵ). In each panel, the pigment pool represents the light-harvesting capacity for the ensemble of photosynthetic units, and it varies in parallel with the sum reductant requirements for nitrogen assimilation (N), carbon fixation (C), and ATP synthesis (ATP). An increase in light (i.e. from top to bottom) decreases the pigment requirement for a given reductant demand, resulting in E_k -dependent changes in the PE relationship that increase ϵ (i.e. the ratio of C:pigment). A decrease in nutrients (i.e. from left to right) causes a decrease in all three reductant sinks, but the decrease in the ATP sink is proportionately smaller than the decreases in N or C. This nutrient-dependent shift reflects changes in cellular reductant:ATP demands and is proposed here as the basis of E_k -independent variability. Such changes cause ϵ to decrease because the carbon sink (C) is more sensitive to nutrient stress than pigment content, since the latter varies in proportion to the sum of N, C, and ATP. According to this scheme, ϵ is highest under high-light replete-nutrient conditions and lowest under low-light nutrient-limiting conditions.

from the Calvin cycle providing the basal substrate for the myriad metabolic pathways. This paradigm, however, is shifting to one where simple reductants, not carbon products, act as the fundamental currency of plant life. From this vantage, variability in the light reaction components of photosynthesis can be viewed as an index of change in cellular reductant demands, and we can maintain the notion that the chl-normalized light-limited slope for photosynthetic electron transport is relatively constant, with sources of variability that are understood and reasonably constrained (Eq. 5).

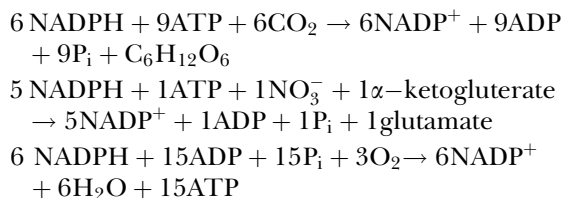
Perhaps our preconception that carbon compounds should be at the base of plant metabolism was influenced by our heterotrophic perspective or the pervasive expression for photosynthesis of



Although such a relationship may function to represent requirements for glucose synthesis, it remains a restrictive definition. More generally, photosynthesis is



This relation provides a more flexible basis for understanding variations in observed carbon fixation and oxygen evolution. The fundamental products of photosynthesis are available for the plant to spend on a variety of secondary pathways, including carbon reduction, nitrogen assimilation, and ATP production:



How the fundamental products of photosynthesis (NADPH, ATP) are distributed among these pathways dictates the apparent light utilization efficiency for carbon fixation (ϵ). Most certainly, this allocation of resources is not stagnant but rather changes constantly across the temporal domain in response to the cell's varied metabolic demands, which imprint changes in external environmental forcings.

We thank Dr. Claudia Steglich, Dr. Wolfgang Hess, and the organizers and participants of OliPac and ProMolec for data and the opportunity to participate in these programs. We thank Drs. Emmanuel Boss and Dan Grzebyk for helpful suggestions on the manuscript. M. Behrenfeld gives special thanks to Elizabeth Stanley for encouragement and understanding and recognizes the pioneering work of Dr. Trevor Platt and colleagues as his original inspiration to investigate the positive correlation issue, which led to the current contribution. This work was supported by the National Aeronautics and Space Administration (RTOP#622-52-58), the National Science Foundation (NSF-INT99-02240), the Ministry of Education of the Czech Republic (LN00A141, MSM 12310001, ME379), the Institutional Research Concept (AV0Z5020903), and a visiting scientist position for O. Prasil provided by the National Research Council. We dedicate this manuscript to Dr. Ivo Šetlik on occasion of his 75th birthday and in recognition

of his decades of interest and research on photosynthesis and the complexities of cell metabolism.

- Adamich, M., Laris P. C. & Sweeney, B. M. 1976. In vivo evidence for a circadian rhythm in membranes of *Gonyaulax*. *Nature* 261:583–5.
- Allali, K., Bricaud, A. & Claustre, H. 1997. Spatial variations in the chlorophyll-specific absorption coefficients of phytoplankton and photosynthetically-active pigments in the equatorial Pacific. *J. Geophys. Res.* 102:12,413–23.
- Alpes, I., Scherer, S. & Böger, P. 1989. The respiratory NADH dehydrogenase of the cyanobacterium *Anabaena variabilis*: purification and characterization. *Biochim. Biophys. Acta* 973:41–6.
- Babin, M., Morel, A. & Gagnon, R. 1994. An incubator designed for extensive and sensitive measurements of phytoplankton photosynthetic parameters. *Limnol. Oceanogr.* 39:694–702.
- Behrenfeld, M. J. & Falkowski, P. G. 1997. A consumer's guide to phytoplankton primary productivity models. *Limnol. Oceanogr.* 42:1479–91.
- Behrenfeld, M. J., Prasil, O., Kolber, Z. S., Babin, M. & Falkowski, P. G. 1998. Compensatory changes in photosystem II electron turnover rates protect photosynthesis from photoinhibition. *Photosynth. Res.* 58:259–68.
- Behrenfeld, M. J. & Kolber, Z. S. 1999. Widespread iron limitation of phytoplankton in the south Pacific ocean. *Science* 283:840–3.
- Behrenfeld, M. J., Randerson, J., McClain, C., Feldman, G., Los, S., Tucker, C., Falkowski, P., Field, C., Frouin, R., Esaias, W., Kolber, D. & Pollack, N. 2001. Biospheric primary production during an ENSO transition. *Science* 291:2594–7.
- Behrenfeld, M. J., Esaias, W. E. & Turpie, K. 2002a. Assessment of primary production at the global scale. In Williams, P. J., Thomas, D. N. & Reynolds, C. S. [Eds.] *Phytoplankton Productivity: Carbon Assimilation in Marine and Freshwater Ecosystems*. Blackwell, Oxford, pp. 156–86.
- Behrenfeld, M. J., Marañón, E., Siegel, D. A. & Hooker, S. B. 2002b. A photoacclimation and nutrient based model of light-saturated photosynthesis for quantifying oceanic primary production. *Mar. Ecol. Prog. Ser.* 228:103–17.
- Behrenfeld, M. J. & Boss, E. 2003. The beam attenuation to chlorophyll ratio: an optical index of phytoplankton physiology in the surface ocean? *Deep Sea Res.* 50:1537–49.
- Bennoun, P. 1982. Evidence for a respiratory chain in the chloroplast. *Proc. Natl. Acad. Sci. USA* 79:4352–6.
- Berges, J. A., Cochlan, W. P. & Harrison, P. J. 1995. Laboratory and field responses of algal nitrate reductase to diel periodicity in irradiance, nitrate exhaustion, and the presence of ammonium. *Mar. Ecol. Progr. Ser.* 124:259–69.
- Birch, D. G., Elrifi, I. R. & Turpin, D. H. 1986. Nitrate and ammonium induced photosynthetic suppression in N-limited *Selenastrum minutum*. II. Effects of NO_3^- and NH_4^+ addition on CO_2 efflux in the light. *Plant Physiol.* 82:708–12.
- Birmingham, B. C., Coleman J. R. & Colman, B. 1982. Measurements of photorespiration in algae. *Plant Physiol.* 69:259–62.
- Björkman, O. 1981. Responses to different quantum flux densities. In Lange, O. L., Nobel, P. S., Osmond, C. B. & Ziegler, H. [Eds.] *Physiological Plant Ecology. I. Responses to the Physical Environment*. Springer-Verlag, Berlin, pp. 57–107.
- Bruyant, F., Babin, M., Sciandra, A., Marie, D., Genty, B., Claustre, H., Blanchot, J., Bricaud, A., Rippka, R., Boulben, S., Louis, F. & Partensky, F. 2001. An axenic cyclostat of *Prochlorococcus* strain PCC9511 with a simulator of natural light regimes. *J. Appl. Phycol.* 13:135–42.
- Champigny, M. -L. 1995. Integration of photosynthetic carbon and nitrogen metabolism in higher plants. *Photosynth. Res.* 46: 117–27.
- Claustre, H., Moline, M. & Prézélin, B. B. 1997. Sources of variability in the column photosynthetic cross section for Antarctic coastal waters. *J. Geophys. Res.* 102:25,047–60.
- Claustre, H., Morel, A., Babin, M., Cailliau, C., Marie, D., Marty, J.-C., Tailliez, D. & Vaulot, D. 1999. Variability in particle

- attenuation and chlorophyll fluorescence in the tropical Pacific: scales, patterns, and biogeochemical implications. *J. Geophys. Res.* 104:3401–22.
- Côté, B. & Platt, T. 1983. Day-to-day variations in the spring-summer photosynthetic parameters of coastal marine phytoplankton. *Limnol. Oceanogr.* 28:320–44.
- Crofts, A. R., Baroli, I., Kramer, D. & Taoka, S. 1993. Kinetics of electron-transfer between Q(A) and Q(B) in wild-type and herbicide-resistant mutants of *Chlamydomonas reinhardtii*. *Z. Naturforsch.* 48c:259–66.
- Cuhel, R. L., Ortner, P. B. & Lean, D. R. S. 1984. Night synthesis of protein by algae. *Limnol. Oceanogr.* 29:731–44.
- Dandonneau, Y. 1999. Introduction to special section: biogeochemical conditions in the equatorial Pacific in late 1994. *J. Geophys. Res.* 104:3291–5.
- Doty, M. S. & Oguri, M. 1957. Evidence for a photosynthetic daily periodicity. *Limnol. Oceanogr.* 2:37–40.
- Elrifi, I. R. & Turpin, D. H. 1986. Nitrate and ammonium induced photosynthetic suppression in N-limited *Selenastrum minutum*. *Plant Physiol.* 81:273–9.
- Elrifi, I. R. & Turpin, D. H. 1987. The path of carbon flow during NO_3^- induced photosynthetic suppression in N-limited *Selenastrum minutum*. *Plant Physiol.* 83:97–104.
- Elrifi, I. R., Holmes, J. J., Weger, H. G., Mayo, W. P. & Turpin, D. H. 1988. RuBP limitation of photosynthetic carbon fixation during NH_3 assimilation. Interaction between photosynthesis, respiration, and ammonium assimilation in N-limited green algae. *Plant Physiol.* 87:395–401.
- Egneus, H., Heber, U., Matthiesen, U. & Kirk, M. 1975. Reduction of oxygen by the electron transport chain of chloroplasts during assimilation of carbon dioxide. *Biochim. Biophys. Acta* 408:252–68.
- Erga, S. R. & Skjoldal, H. R. 1990. Diel variations in photosynthetic activity of summer phytoplankton in Lindåspollene, western Norway. *Mar. Ecol. Prog. Ser.* 65:73–85.
- Escoubas, J., Lomas, M., LaRoche, J. & Falkowski, P. 1995. Light intensity regulation of *cab* gene transcription is signaled by the redox state of the plastoquinone pool. *Proc. Natl. Acad. Sci. USA* 92:10237–41.
- Fleischhacker, P. & Senger, H. 1978. Adaptation of the photosynthetic apparatus of *Scenedesmus obliquus* to strong and weak light conditions. II. Differences in photochemical reactions, the photosynthetic electron transport and photosynthetic units. *Physiol. Plant.* 43:43–51.
- Field, C. B., Behrenfeld, M. J., Randerson, J. T. & Falkowski, P. G. 1998. Primary production of the biosphere: integrating terrestrial and oceanic components. *Science* 281:237–40.
- Flynn, K. J. 2001. A mechanistic model for describing dynamic multi-nutrient, light, temperature interactions in phytoplankton. *J. Plankton Res.* 23:977–97.
- Flynn, K. J., Marshall, H. & Geider, R. J. 2001. A comparison of two N-irradiance interaction models of phytoplankton growth. *Limnol. Oceanogr.* 46:1794–802.
- Forbes, J. R., Denman, K. L. & Mackas, D. L. 1986. Determinations of photosynthetic capacity in coastal marine phytoplankton: effects of assay irradiance and variability of photosynthetic parameters. *Mar. Ecol. Prog. Ser.* 32:181–91.
- Gao, Y., Smith, G. J. & Alberte, R. S. 1992. Light regulation of nitrate reductase in *Ulva-Fenestrata* (Chlorophyceae). 1. Influence of light regimes on nitrate reductase activity. *Mar. Biol.* 112:691–6.
- Gardstrom, P. & Lernmark, U. 1995. The contribution of mitochondria to energetic metabolism in photosynthetic cells. *J. Bioenerg. Biomembr.* 27:415–21.
- Geider, R. J., MacIntyre, H. L. & Kana, T. 1996. A dynamic model of photoacclimation in phytoplankton. *Limnol. Oceanogr.* 41:1–15.
- Geider, R. J., MacIntyre, H. L. & Kana, T. 1998. A dynamic regulatory model of phytoplanktonic acclimation to light, nutrients, and temperature. *Limnol. Oceanogr.* 43:679–94.
- Geider, R. J. & MacIntyre, H. L. 2002. Physiology and biochemistry of photosynthesis and algal carbon acquisition. In Williams, P. J., Thomas, D. N. & Reynolds, C. S. [Eds.] *Phytoplankton Productivity: Carbon Assimilation in Marine and Freshwater Ecosystems*. Blackwell, Oxford, pp. 44–77.
- Harding, L. W. Jr, Meeson, B. W., Prézelin, B. B. & Sweeney, B. M. 1981a. Diel periodicity of photosynthesis in marine phytoplankton. *Mar. Biol.* 61:95–105.
- Harding, L. W., Prézelin, B. B., Sweeney, B. M. & Cox, J. L. 1981b. Diel oscillations in the photosynthesis-irradiance relationship of a planktonic marine diatom. *J. Phycol.* 17:389–94.
- Harding, L. W., Jr., Prézelin, B. B., Sweeney, B. M. & Cox, J. L. 1982. Diel oscillations of the photosynthesis-irradiance (P-I) relationship in natural assemblages of phytoplankton. *Mar. Biol.* 67:167–78.
- Harding, L. W., Jr., Meeson, B. W. & Fisher, T. R. 1985. Photosynthesis patterns in Chesapeake Bay phytoplankton: short- and long-term responses of P-I curves to light. *Mar. Ecol. Prog. Ser.* 26:99–111.
- Harding, L. W. Jr., Meeson, B. W. & Fisher, T. R. 1986. Phytoplankton production in two East coast estuaries: photosynthesis-light functions and patterns of carbon assimilation in Chesapeake and Delaware Bays. *Est. Coast. Shelf Sci.* 23:773–806.
- Harding, L. W. Jr., Fisher, T. R. & Tyler, M. A. 1987. Adaptive responses of photosynthesis in phytoplankton: specificity to time-scale of change in light. *Biol. Oceanogr.* 4:403–37.
- Hastings, J. W., Astrachan, L. & Sweeney, B. M. 1961. A persistent daily rhythm in photosynthesis. *J. Cell. Physiol.* 45:69–76.
- Heber, U. 1974. Metabolite exchange between chloroplasts and cytoplasm. *Annu. Rev. Plant Physiol. Plant Mol. Biol.* 25:393–421.
- Heber, U., Neimanis, S. & Dietz, K.-J. 1988. Fractional control of photosynthesis by the Q_B protein, the cytochrome *f/b_6* complex and other components of the photosynthetic apparatus. *Planta* 173:267–74.
- Heineke, D., Riens, B., Grosee, H., Hoferichter, P., Peter, U., Flugge, U. I. & Heldt, H. W. 1991. Redox transfer across the inner chloroplast envelope membrane. *Plant Physiol.* 95:1131–7.
- Heldt, H. W., Heineke, D., Heupel, R., Krömer, S. & Riens, B. 1990. Transfer of redox equivalents between subcellular compartments of a leaf cell. In Batscheffsky, M. [Ed.] *Current Research in Photosynthesis*. Kluwer, Dordrecht, The Netherlands, pp. 1.5–7.
- Hellebust, J. & Terborgh, J. 1967. Effects of environmental conditions on rate of photosynthesis and some photosynthetic enzymes in *Dunaliella tertiolecta* Butcher. *Limnol. Oceanogr.* 12:559–67.
- Hellebust, J., Terborgh, J. & McLeod, G. C. 1967. Photosynthetic rhythm of *Acetabularia crenulata*. 2. Measurements of photo-assimilation of carbon dioxide and activities of enzymes of reductive pentose cycle. *Biol. Bull.* 133:670:5.
- Henley, W. J. 1993. Measurement and interpretation of photosynthetic light response curves in algae in the context of photoinhibition and diel changes. *J. Phycol.* 29:729–39.
- Henley, W. J., Levavasseur, G., Franklin, L. A., Lindley, S. T., Rasmus, J. & Osmond, C. B. 1991. Diurnal responses of photosynthesis and fluorescence in *Ulva rotundata* acclimated to sun and shade in outdoor culture. *Mar. Ecol. Progr. Ser.* 75:19–28.
- Herman, E. M. & Sweeney, B. M. 1975. Circadian rhythm of chloroplast ultrastructure in *Gonyaulax-Polyedra*, concentric organization around a central cluster of ribosomes. *J. Ultrastruct. Res.* 50:347–54.
- Hoefnagel, M. H. N., Atkin, O. K. & Wiskich, J. T. 1998. Interdependence between chloroplasts and mitochondria in the light and the dark. *Biochim. Biophys. Acta* 1366:235–55.
- Jassby, A. D. & Platt, T. 1976. Mathematical formulation of the relationship between photosynthesis and light for phytoplankton. *Limnol. Oceanogr.* 21:540–7.
- Kaftan, D., Meszaros, T., Whitmarsh, J. & Nedbal, L. 1999. Characterization of photosystem II activity and heterogeneity during the cell cycle of the green alga *Scenedesmus quadricauda*. *Plant Physiol.* 120:433–41.

- Kana, T. M. 1992. Relationship between photosynthetic oxygen cycling and carbon assimilation in *Synechococcus* WH7803 (Cyanophyta). *J. Phycol.* 28:304–8.
- Kok, B. 1956. On the inhibition of photosynthesis by intense light. *Biochim. Biophys. Acta* 21:234–44.
- Leverenz, J. W., Falk, S., Pilstrom, C. -M. & Samuelsson, G. 1990. The effects of photoinhibition on the photosynthetic light-response curve of green plant cells (*Chlamydomonas reinhardtii*). *Planta* 182:161–8.
- Li, W. K. W., Glover, H. E. & Morris, I. 1980. Physiology of carbon photoassimilation by *Oscillatoria thiebautii* in the Caribbean Sea. *Limnol. Oceanogr.* 25:447–56.
- Liu, H., Landry, M. R., Vault, D. & Campbell, L. 1999. *Prochlorococcus* growth rates in the central equatorial Pacific: an application of the f_{max} approach. *J. Geophys. Res.* 104:3391–9.
- Loneragan, T. A. & Sargent, M. L. 1979. Regulation of the photosynthesis rhythm in *Euglena gracilis*. 2. Involvement of electron flow through both photosystems. *Plant Physiol.* 64:99–103.
- MacIntyre, H. L., Kana, T. M., Anning, T. & Geider, R. J. 2002. Photoacclimation of photosynthesis irradiance response curves and photosynthetic pigments in microalgae and cyanobacteria. *J. Phycol.* 38:17–38.
- Malkin, R. & Niyogi, K. 2000. Photosynthesis. In Buchanan, B., Gruissem, W. & Jones, R. [Eds.] *Biochemistry and Molecular Biology of Plants*. American Society of Plant Physiologists, John Wiley and Sons, Inc. Somerset, New Jersey, USA, pp. 568–628.
- Marcus, Y., Schuster, G., Michaels, A. & Kaplan, A. 1986. Adaptation to CO₂ levels and changes in the phosphorylation of thylakoid proteins during the cell cycle of *Chlamydomonas reinhardtii*. *Plant Physiol.* 80:604–7.
- Mishkind, M., Mauzerall, D. & Beale, S. I. 1979. Diurnal variations in situ of photosynthetic capacity in *Ulva* caused by a dark reaction. *Plant Physiol.* 64:896–9.
- Moline, M. A., Schofield, O. & Boucher, N. P. 1998. Photosynthetic parameters and empirical modeling of primary production: a case study on the Antarctic peninsula shelf. *Antarctic Sci.* 10:45–54.
- Morales, F., Abadia, A. & Abadia, J. 1991. Chlorophyll fluorescence and photon yield of oxygen evolution in iron deficient sugar beet (*Beta vulgaris* L.) leaves. *Plant Physiol.* 97:866–93.
- Myers, J. & Graham, J. R. 1975. Photosynthetic unit size during synchronous life cycle of *Scenedesmus*. *Plant Physiol.* 55:686–8.
- Nara, M., Shiraiwa, Y. & Hirokawa, T. 1989. Changes in the carbonic anhydrase activity and the rate of photosynthetic O₂ evolution during the cell cycle of *Chlorella ellipsoidea* C-27. *Plant Cell Physiol.* 30:267–75.
- Noctor, G. & Foyer, C. H. 2000. Homeostasis of adenylate status during photosynthesis in a fluctuation environment. *J. Exp. Bot.* 51:347–56.
- Orellana, M. V. & Perry, M. J. 1992. An immunoprobe to measure Rubisco concentrations and maximal photosynthesis rates of individual phytoplankton cells. *Limnol. Oceanogr.* 37:978–90.
- Ort, D. R. & Baker, N. R. 2002. A photoprotective role for O₂ as an alternative sink in photosynthesis? *Plant Biol.* 5:193–8.
- Osmond, C. B. 1981. Photorespiration and photosynthesis: some implications for the energetics of photosynthesis. *Biochim. Biophys. Acta* 639:77–98.
- Padmasree, K. & Raghavendra, A. S. 1998. Interaction with respiration and nitrogen metabolism. In Raghavendra, A. S. [Ed.] *Photosynthesis: A Comprehensive Treatise*. Cambridge University Press, Cambridge, UK, pp. 197–211.
- Palmer, J. D., Livingston, L. & Zusy, F. D. 1964. A persistent diurnal rhythm in photosynthetic capacity. *Nature* 203:1087–8.
- Peltier, G. &ournac, L. 2002. Chlororespiration. *Annu. Rev. Plant Biol.* 53:523–50.
- Pfannschmidt, T., Nilsson, A. & Allen, J. F. 1999. Photosynthetic control of chloroplast gene expression. *Nature* 397:625–8.
- Platt, T. & Jassby, A. D. 1976. The relationship between photosynthesis and light for natural assemblages of coastal marine phytoplankton. *J. Phycol.* 12:421–30.
- Platt, T., Sathyendranath, S., Ulloa, O., Harrison, W. G., Hoepffner, N. & Goes, J. 1992. Nutrient control of phytoplankton photosynthesis in the Western North Atlantic. *Nature* 356:229–31.
- Post, A. F., Eijgenraam, F. & Mur, L. R. 1985. Influence of light period length on photosynthesis and synchronous growth of the green alga *Scenedesmus protuberans*. *Br. Phycol. J.* 20:391–7.
- Prasil, O., Kolber, Z., Berry, J. A. & Falkowski, P. G. 1996. Cyclic electron flow around photosystem-II in-vivo. *Photosynth. Res.* 48:395–410.
- Prézelin, B. B. 1992. Diel periodicity in phytoplankton productivity. *Hydrobiologia* 238:1–35.
- Prézelin, B. B. & Sweeney, B. M. 1977. Characterization of photosynthetic rhythms in marine dinoflagellates. 2. Photosynthesis-irradiance curves and in vivo chlorophyll a fluorescence. *Plant Physiol.* 60:388–92.
- Putt, M. & Prézelin, B. B. 1988. Diel periodicity of photosynthesis and cell division compared in *Thalassiosira weissflogii* (Bacillariophyceae). *J. Phycol.* 24:315–24.
- Raateoja, M. P. & Seppala, J. 2001. Light utilization and photosynthetic efficiency of *Nannochloris* sp. (Chlorophyceae) approached by spectral absorption characteristics and fast repetition rate fluorometry (FRRF). *Boreal Environ. Res.* 6:205–20.
- Raghavendra, A. S., Padmasree, K. & Saradadevi, K. 1994. Interdependence of photosynthesis and respiration in plant cells—interactions between chloroplasts and mitochondria. *Plant Sci.* 97:1–14.
- Raimbault P., Slawyk, G., Boudjellal, B., Coatanoan, C., Conan, P., Coste, B., Garcia, N., Moutin, T. & Pujo-Pay, M. 1999. Carbon and nitrogen uptake and export in the equatorial Pacific at 150 degrees W: evidence of an efficient regenerated production cycle. *J. Geophys. Res.* 104:3341–56.
- Rivkin, R. B. 1990. Photoadaptation in marine phytoplankton: variations in ribulose 1,5-bisphosphate activity. *Mar. Ecol. Prog. Ser.* 62:61–72.
- Samuelsson, G., Sweeney, B. M., Matlick, H. A. & Prézelin, B. B. 1983. Changes in photosystem-II account for the circadian rhythm in photosynthesis in *Gonyaulax polyedra*. *Plant Physiol.* 73:329–31.
- Scherer, S. 1990. Do photosynthetic and respiratory electron transport chains share redox proteins? *Trends Biochem. Sci.* 15:458–62.
- Schmid, G. H. & Gafron, H. 1968. Photosynthetic units. *J. Gen. Physiol.* 52:212–39.
- Senger, H. 1970a. Characterization of a synchronous culture of *Scenedesmus obliquus*, its potential photosynthetic capacity and its photosynthetic quotient during life cycle. *Planta* 90:243–9.
- Senger, H. 1970b. Quantum yield and variable behavior of 2 photosystems of photosynthetic apparatus during life cycle of *Scenedesmus obliquus* in synchronous cultures. *Planta* 92:327–46.
- Senger, H. 1975. Changes in photosynthetic activities in synchronous cultures of *Scenedesmus*, *Chlorella* and *Chlamydomonas*. Les Cycles Cellulaires et Leur Blocage Chez Plusieurs Protistes, Collog. No 240. M. Lefort-Tran and R. Valencia. Paris, CNRS, pp. 101–13.
- Senger, H. & Bishop, N. I. 1967. Quantum yield of photosynthesis in synchronous *Scenedesmus* cultures. *Nature* 214:140–2.
- Siedow, J. N. & Day, D. A. 2000. Respiration and photorespiration. In Buchanan, B., Gruissem, W. & Jones, R. [Eds.] *Biochemistry and Molecular Biology of Plants*. American Society of Plant Physiologists, John Wiley and Sons, Inc. Somerset, New Jersey, USA, pp. 676–728.
- Sorokin, C. & Krauss, R. W. 1961. Relative efficiency of photosynthesis in the course of cell development. *Biochim. Biophys. Acta* 48:314–9.
- Steemann Nielsen, E. & Jørgensen, E. G. 1968. The adaptation of plankton algae. I. General part. *Physiol. Plant.* 21:401–13.
- Steglich, C., Behrenfeld, M. J., Koblizek, M., Claustre, H., Penno, S., Prasil, O., Partensky, F. & Hess, W. R. 2001. Nitrogen deprivation strongly affects photosystem II but not phycoerythrin level in the chlorophyll *b*-possessing cyanobacterium *Prochlorococcus marinus*. *Biochim. Biophys. Acta* 1503:341–9.

- Sukenik, A., Bennett, J. & Falkowski, P. G. 1987. Light-saturated photosynthesis—limitation by electron transport or carbon fixation? *Biochim. Biophys. Acta* 891:205–15.
- Sweeney, B. M., Prézelin, B. B., Wong, D. & Govindjee, D. 1979. In vivo chlorophyll-a fluorescence transients and the circadian rhythm of photosynthesis in *Gonyaulax polyedra*. *Photochem. Photobiol.* 30:309–11.
- Talling, J. F. 1957. The phytoplankton population as a compound photosynthetic system. *New Phytol.* 56:133–49.
- Terborgh, J. & McLeod, G. C. 1967. Photosynthetic rhythm of *Acetabularia crenulata*. I. Continuous measurements of oxygen exchange in alternating light-dark regimes and in constant light of different intensities. *Biol. Bull.* 133:659–67.
- Turpin, D. H. 1991. Effects of inorganic N availability on algal photosynthesis and carbon metabolism. *J. Phycol.* 27:14–20.
- Vaulot, D. & Marie, D. 1999. Diel variability of photosynthetic pico-plankton in the equatorial Pacific. *J. Geophys. Res.* 104:3297–310.
- Vergara, J. J., Berges, J. A. & Falkowski, P. G. 1998. Diel periodicity of nitrate reductase activity and protein levels in the marine diatom *Thalassiosira weissflogii* (Bacillariophyceae). *J. Phycol.* 34:952–61.
- Weger, H. G., Birch, D. G., Elrifi, I. R. & Turpin, D. H. 1988. Ammonium assimilation requires mitochondrial respiration in the light: a study with the green alga *Selenastrum minutum*. *Plant Physiol.* 86:688–92.
- Weger, H. G., Herzig, R., Falkowski, P. G. & Turpin, D. H. 1989. Respiratory losses in the light in a marine diatom: measurements by short-term mass spectrometry. *Limnol. Oceanogr.* 34:1153–61.
- Weger, H. G. & Turpin, D. H. 1989. Mitochondrial respiration can support NO_3^- and NO_2^- reduction during photosynthesis: interactions between photosynthesis, respiration, and N assimilation in the N-limited green alga *Selenastrum minutum*. *Plant Physiol.* 89:409–15.
- Weinbaum, S. A., Gressel, J., Reisfeld, A. & Edelman, M. 1979. Characterization of the 32,000 Dalton chloroplast membrane protein: probing its biological function in *Spirodela*. *Plant Physiol.* 64:828–32.
- Wilhelm, C. & Wild, A. 1984. The variability of the photosynthetic unit in *Chlorella*: the effect of light intensity and cell development on photosynthesis, P-700 and cytochrome f in homo-continuous and synchronous cultures of *Chlorella*. *J. Plant. Physiol.* 115:125–35.